0888-8809/08/$15.00/0
Printed in U.S.A.

Molecular Endocrinology 22(4):838–857

doi: 10.1210/me.2007-0218

The Phytoestrogen Coumestrol Is a Naturally Occurring Antagonist of the Human Pregnane X Receptor

Hongwei Wang,* Hao Li,* Linda B. Moore,* Michael D. L. Johnson, Jodi M. Maglich, Bryan Goodwin, Olivia R. R. Ittoop, Bruce Wisely, Katrina Creech, Derek J. Parks, Jon L. Collins, Timothy M. Willson, Ganjam V. Kalpana, Madhukumar Venkatesh, Wen Xie, Sool Y. Cho, John Roboz, Matthew Redinbo, John T. Moore, and Sridhar Mani

Albert Einstein College of Medicine, Albert Einstein Cancer Center (H.W., H.L., S.M.), Departments of Medicine (H.W., H.L., S.M.) and Molecular Genetics (G.V.K., M.V.), Bronx, New York 10461; Molecular Discovery Research (L.B.M., J.M.M., B.G., O.R.R.I., B.W., K.C., D.J.P., J.L.C., T.M.W., J.T.M.), GlaxoSmithKline, Research Triangle Park, North Carolina 27709; University of North Carolina (M.D.L.J., M.R.), Chapel Hill, North Carolina 27599; University of Pittsburgh (W.X.), Pittsburgh, Pennsylvania 15261; and Mount Sinai School of Medicine (S.Y.C., J.R.), New York, New York 10029

Antagonizing the action of the human nuclear xenobiotic receptor pregnane X receptor (PXR) may have important clinical implications in preventing drug-drug interactions and improving therapeutic efficacy. We provide evidence that a naturally occurring phytoestrogen, coumestrol, is an antagonist of the nuclear receptor PXR (NR1I2). In transient transfection assays, coumestrol was able to suppress the agonist effects of SR12813 on human PXR activity. PXR activity was assessed and correlated with effects on the metabolism of the anesthetic tribromoethanol and on gene expression in primary human hepatocytes. We found that coumestrol was able to suppress the effects of PXR agonists on the expression of the known PXR target genes, *CYP3A4* and *CYP2B6,* in primary human hepatocytes as well as inhibit metabolism of tribromoethanol in humanized PXR mice. Coumestrol at concentrations above 1.0 μM competed in scintillation proximity assays with a labeled PXR agonist for binding to the ligand-binding cavity. However, mammalian two-hybrid assays and transient transcription data using ligand-binding-cavity mutant forms of PXR show that coumestrol also antagonizes coregulator recruitment. This effect is likely by binding to a surface outside the ligand-binding pocket. Taken together, these data imply that there are antagonist binding site(s) for coumestrol on the surface of PXR. These studies provide the basis for development of novel small molecule inhibitors of PXR with the ultimate goal of clinical applications toward preventing drug-drug interactions. (*Molecular Endocrinology* 22: 838–857, 2008)

THE NUCLEAR RECEPTOR pregnane X receptor (PXR, NR1I2) has been shown to be activated by a chemically and structurally diverse set of xenobiotic and endogenous compounds (1–6). PXR regulates gene expression pathways involved in metabolism and transport of these same classes of compounds (8). Notably, PXR has been shown to directly regulate the *cytochrome P450 3A* gene, a phase I drug metabolism gene whose product is responsible for oxidative metabolism of more than 50% of all drugs. Consistent with the function of PXR as a xenobiotic sensor, virtually all PXR ligands isolated to date demonstrated agonist activity. A large set of xenobiotics, bile acids, steroids, and benzoate molecules were tested against PXRs from multiple species in transient transfection and all of the compounds, if active, were agonists (9–13). A dilemma in this field is how PXR is capable of being activated by such a diverse range of compounds. Two extreme examples include the relatively small [β-estradiol with molecular weight (MW) of 272.4] and the large macrolide antibiotic rifampicin (MW 822.9) (9–12).

Part of the answer to this dilemma has come from structural studies of the human PXR ligand-binding domain (LBD). The crystal structure of the PXR LBD

First Published Online December 20, 2007

* H.W., H.L., and L.B.M. contributed equally to this work.

Abbreviations: AR, Androgen receptor; CAR, constitutive androstane receptor; DMSO, dimethylsulfoxide; ER, estrogen receptor; ET-743, ecteinascidin-743; FP, fluorescence polarization; FXR, farnesoid X receptor; β-gal, β-galactosidase; GFP, green fluorescent protein; GR, glucocorticoid receptor; H&E, hematoxylin and eosin; LBD, ligand-binding domain; LORR, loss of righting reflex; LXR, liver X receptor; MBP, maltose-binding protein; MR, mineralocorticoid receptor; MW, molecular weight; NMTB, *N*-methyl-*N*-[4-[2,2,2-trifluoro-1-hydroxy-1-(trifluoromethyl) ethyl]phenyl]benzenesulfonamide; PCN, pregnenolone carbonitrile; PPAR, peroxisome proliferator activator receptor; PXR, pregnane X receptor; RAR, retinoic acid receptor; RXR, retinoid X receptor; SPA, scintillation proximity assay; SRC-1, steroid receptor coactivator-1; T1317, T0901317; TR, thyroid hormone receptor; VDR, vitamin D receptor.

***Molecular Endocrinology* is published monthly by The Endocrine Society (http://www.endo-society.org), the foremost professional society serving the endocrine community.**

was solved in the apo form or in a complex with SR12813 (13). The structure revealed a large spherical but elongated ligand-binding cavity lined with a small number of polar residues. The combination of these features explained how the LBD could accommodate a diverse array of molecules. The promiscuous nature of the ligand-binding pocket was exemplified by the fact that SR12813 could bind in the pocket in three orientations. In both the apo and SR12813 crystallographic structures of PXR, the AF-2 helix was in the active conformation (13). More recently, the crystal structure of PXR LBD in complex with another nanomolar potency ligand, T0901317 (T1317), has been solved. These investigators were successful in generating PXR-specific ligand analogs of T1317 [because this compound also acts as a liver X receptor (LXR) agonist]; however, they could not generate antagonists targeting the ligand-binding pocket. They argued that this was difficult due to PXR's ligand pocket promiscuity and structural conformability (15). In this regard, it is crucial to note that this very promiscuous nature of the ligand-binding pocket allows for structurally related compounds that can bind to the pocket in distinct modes (10). For example, 17β-estradiol binds to PXR leaving a 1000-Å (3) space in the ligand-binding pocket that is unoccupied. Therefore, structurally similar or dissimilar small molecules may actually fit into this pocket and exert agonist/antagonist properties (9). This example is best shown for the estrogen receptor (ER), because estrogen, diethylstilbestrol (an analog), and 4-hydroxytamoxifen can bind to the ligand-binding pocket in distinct modes (16).

A key feature of nuclear receptor activation is the ability of an agonist to stabilize the active state of the terminal helix in the LBD, which creates the surface AF-2 site. This domain interacts directly with transcriptional coactivators to mediate the up-regulation of gene expression. Disruption of the position of the terminal helix 12 in the LBD of the estrogen and estrogen-related receptors is the molecular basis for the antagonist action of tamoxifen and related anticancer drugs (*e.g.* 4-hydroxytamoxifen) used to treat breast carcinomas (17, 18). Recently, this concept has been extended to discovery of novel small molecule inhibitors of the thyroid receptor (19).

PXR antagonists would be useful to study the molecular basis of receptor function. In addition, in clinical settings, they may prevent drug-drug interactions and tune the efficacy of therapeutics that serve as PXR agonists. To date, only three PXR antagonists have been described: ketoconazole (and related azoles) (18), suphoraphane (20), and ecteinascidin-743 (ET-743) (21). Ketoconazole was first described as a PXR antagonist by Takeshita *et al.* (22) and was subsequently shown to disrupt the binding of coregulators (including both coactivators and corepressors) to the surface of PXR in an agonist-dependent fashion (23). For example, in the presence of the established PXR activator rifampicin, ketoconazole and related azoles were shown to prevent the activation of the receptor both *in vitro* in cell-based assays and in humanized PXR mouse models (15). Furthermore, our laboratory has shown that ketoconazole binds to at least a region outside the ligand-binding pocket. We have shown using genetic means that the revertant AF-2 region double mutant of PXR (T248E/K277Q) activates with rifampicin but is not inhibited by ketoconazole (18). These data establish that small-molecule modulators can antagonize PXR and that the surface AF-2 site of the receptor appears to be a target of such compounds. ET-743 was reported to act as a PXR antagonist; however, the utility of ET-743 as a chemical tool is limited by the fact that it is not readily available (21).

Coumestrol is a member of the isoflavonoid family, a plant-derived compound with estrogen-like structure and actions (Fig. 1A). Animal studies have shown that phytoestrogens, including coumestrol, invoke a wide range of biological effects, many of which are related to its effects on ERα and -β (24). We have undertaken a study to profile the effects of coumestrol on receptors within the human nuclear receptor superfamily. These studies have ultimately led us to identify coumestrol as a novel and naturally occurring antagonist of the nuclear xenobiotic receptor PXR. We show that coumestrol has at least one binding site for an antagonist outside that ligand-binding pocket.

RESULTS

Transient Transfection Assays

To assess potential nuclear receptor ligands, we have generated a panel of transient transfection functional assays for nuclear receptors that are currently known to be ligand regulated. These receptors include the androgen receptor (AR, NR3C4), progesterone receptor (PR, NR3C3), glucocorticoid receptor (GR, NR3C1), ERα and -β (NR3A1/3A2), mineralocorticoid receptor (MR, NR3C2), retinoic acid receptor α (RARα, NR1B1), PXR (NR1I2), constitutive androstane receptor (CAR, NR1I3), retinoid X receptor α (RXRα, NR2B1), thyroid hormone receptors α and β (TRα/β, NR1A1/1A2), vitamin D receptor (VDR, NR1I1), farnesoid X receptor (FXR, NR1H4), LXRα and -β (NR1H3/1H2), and peroxisome proliferator activator receptors α, γ, and δ (PPARα/γ/δ, NR1C1/1C2/1C3). More information on the nomenclature of these receptors can be found at http://www.ens-lyon.fr/LBMC/laudet/nomenc.html. The assays were performed in CV-1 or T47D cells (for the ERs) using gal4 chimera constructs (FXR, LXRα and -β, RARα, VDR, TRα and -β, and PPARα, δ, and γ) or full-length nuclear receptor expression constructs (GR, PR, AR, MR, ERα and -β, RXRα, PXR, and CAR) in combination with a reporter vector containing relevant regulatory sites. Positive control agonists for each receptor were included in parallel in each respective assay (data not shown).

The phytoestrogen coumestrol (Fig. 1A) was tested for activity in this panel of nuclear receptor assays at a

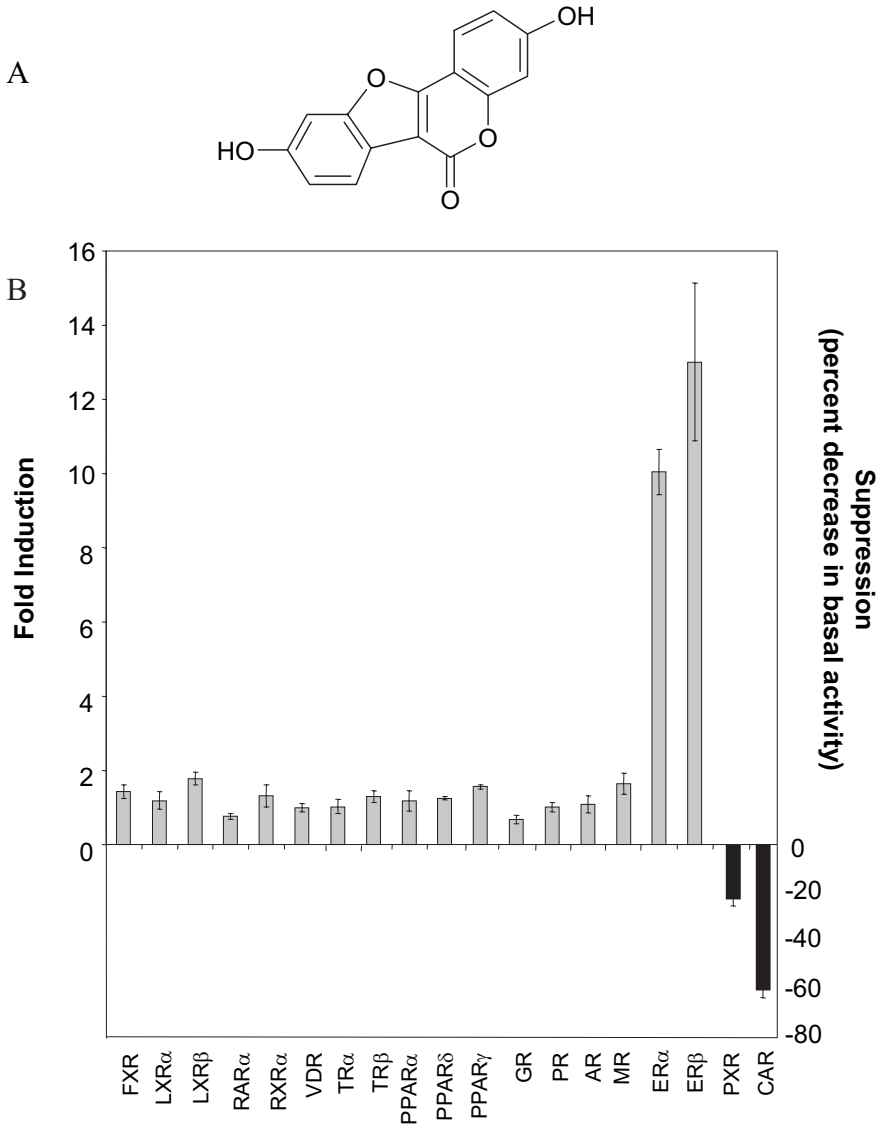

Fig. 1. Effects of Coumestrol on Nuclear Receptor Activity

A, Structure of the phytoestrogen coumestrol; B, coumestrol activity was assessed across a broad panel of nuclear receptors. Coumestrol was tested at 25 μM and activity plotted as either fold induction relative to basal activity (*left axis*) or as percentage decrease in basal activity (*right axis*).

dose of 25 μM. Coumestrol was inactive as an agonist on all nuclear receptors tested except ERα and ERβ (Fig. 1B). In full dose-response curves, coumestrol exhibited EC_{50} values of 67 and 21 nM on ERα and ERβ, respectively (data not shown), consistent with literature values. Although inactive as an inverse agonist on other nuclear receptors, coumestrol suppressed reporter activity in the PXR and CAR assays. Specifically, coumestrol (25 μM) decreased the basal expression of the reporter used in the PXR transient transfection assays by 20% and the CAR basal activity by 60% (Fig. 1B). Multiple inverse agonists have been previously identified for CAR, such as androstanol (25) and multiple bile acids (26). Thus, we focused subsequent studies on providing further characterization of the antagonist effects of coumestrol on PXR.

Coumestrol and its analogs, coumestrol diacetate and coumestrol dimethyl ether, were tested for effects on mouse PXR at a dose of 25 μM. Coumestrol slightly (by 5%) increased the basal expression of the reporter used in the PXR transfection assays. In contrast to that seen with human PXR, coumestrol does not antagonize pregnenolone carbonitrile (PCN)-mediated PXR activation ($P > 0.08$; Fig. 2A). We next tested whether the related compounds coumestrol diacetate and coumestrol dimethyl ether could serve as PXR antagonists. Both coumestrol analogs increased the basal expression of the reporter by 100 and 120%, respectively. However, the analogs did not antagonize PCN-mediated activation of PXR (Fig. 2A). These experiments provide evidence that coumestrol does not antagonize mouse PXR. In human PXR transfection

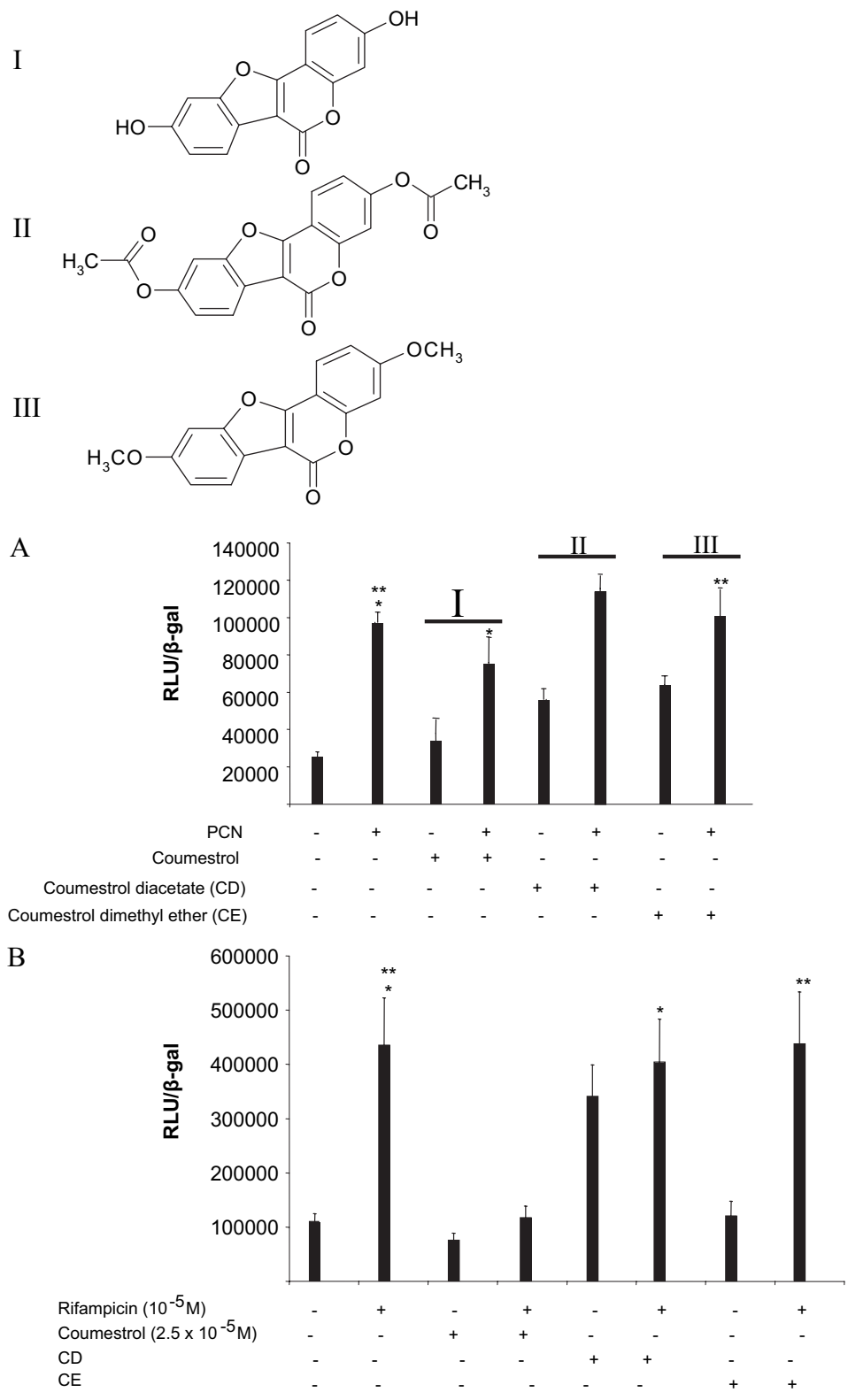

Fig. 2. Effects of Coumestrol Analogs on PXR Activity

CV-1 cells were transfected with mouse PXR (pSG5 plasmid) (A) or human PXR (B) and XREM-tk-luciferase reporter vector. Cell extracts were assayed for luciferase activity after drug treatment for 43 h. Drugs included PCN (10 μM), coumestrol (I), coumestrol diacetate (CD) (II), and coumestrol ester (CE) (III) (25 μM each) alone or in combination with PCN. For the human PXR transfection studies, the drugs included rifampicin (10 μM), coumestrol (25 μM), coumestrol diacetate, or coumestrol ester (25 μM each) alone or in combination with rifampicin. Data for each *column* represent the mean of three independent assays performed in triplicate ± SE. *, $P > 0.08$; **, $P > 0.1$.

assays, coumestrol inhibited rifampicin-mediated activation of PXR (Fig. 2B). Coumestrol diacetate activated human PXR and did not antagonize rifampicin-mediated PXR activation ($P > 0.08$; Fig. 2B). Similarly, coumestrol dimethyl ether also did not antagonize rifampicin-mediated PXR activation ($P > 0.1$; Fig. 2B). These experiments provide evidence that coumestrol antagonizes human PXR but not mouse PXR.

We next conducted a complete dose-response curve for coumestrol using transiently transfected cells (Fig. 3). The full-length human PXR transient transfection assay used the XREM-luciferase reporter vector (see *Materials and Methods*). Antagonist assays were carried out in the presence of the PXR agonist SR12813 (300 nM, a dose that resulted in ~70% of maximal reporter activity). This assay demonstrated that coumestrol was an effective human PXR antagonist and had an IC_{50} value of 12 μM on PXR (Fig. 3A). At the highest concentrations, PXR activity could be completely abolished by coumestrol. In the CAR inverse agonist assay, coumestrol demonstrated an EC_{50} of 29.6 μM (Fig. 3B).

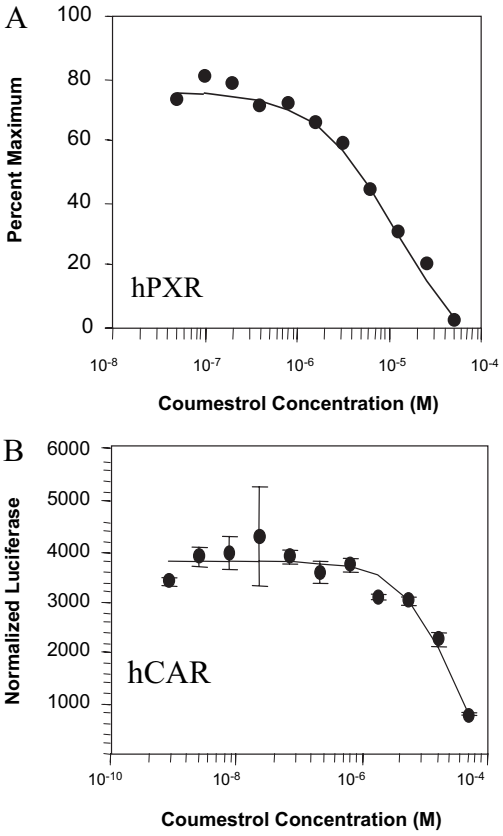

Fig. 3. Effect of Coumestrol on PXR and CAR Activity

CV-1 cells were transfected with expression plasmids for human PXR (A) or human CAR (B) and the XREM-tk-Luciferase reporter vector. Cell extracts were assayed for luciferase activity after compound treatment for 24 h. In the PXR antagonist assay, 300 nM SR12813 was added to increase the basal activity of the reporter to approximately 70% of maximal activity. A full dose-response curve is shown for coumestrol in this assay. Data at each point represent the means of assays performed in triplicate and are plotted relative to the maximal response relative to SR12813 (the ±SE was less than 0.05% for all data points plotted). The mean IC_{50} of coumestrol was 11.6 μM for PXR in these assays. In the CAR inverse agonist assay (did not require addition of agonist to increase basal activity), coumestrol demonstrated an EC_{50} of 29.6 μM.

Competition Binding Assays

We next tested whether coumestrol mediates its antagonist effects through direct binding to PXR. To evaluate PXR binding, we used an established competition binding assay (27) with [^{3}H]*N*-methyl-*N*-[4-[2,2,2-trifluoro-1-hydroxy-1-(trifluoromethyl) ethyl]phenyl]benzenesulfonamide ([^{3}H]NMTB) as a radioligand. When the PXR agonist SR12813 was tested in this assay, a K_i of 37 nM was observed (Fig. 4A). When coumestrol was tested in this assay, a K_i of 13 μM was observed (Fig. 4A), indicating that coumestrol competes for binding to the LBD of human PXR. The difference in the potency of SR12813 and coumestrol in the binding assay is consistent with their differences in potency in transient transfection assays. To evaluate CAR binding, we used an established scintillation proximity assay (28). When clotrimazole was tested in this assay as a positive control, a K_i of 250 nM was observed (Fig. 4B), in agreement with previously published reports (26). When coumestrol was tested in this assay, a K_i of 54 μM was observed (Fig. 4B), indicating that coumestrol competes for binding to the LBD of human CAR. The potency of coumestrol in the binding assay is consistent with its activity in transient transfection assays.

Effect on a Ligand-Binding-Pocket-Filling Mutant of PXR

To assess the impact of the ligand-binding pocket of human PXR on the antagonist potential of coumestrol, we have generated a transient transfection functional assay for the PXR mutant(s) S247W, C284W, and S208W. The S247W mutant was originally described as a pocket-filling mutant, with the serine replaced by a larger tryptophan, that confers a constitutive, ligand-independent activity to PXR (30). These transfection assays were performed in CV-1 cells using either a CYP3A4 (promoter) or MRP2 (promoter) reporter. In CV-1 cells, we tested the effect of coumestrol on the S247W mutant of human PXR (Fig. 5, A and B). Coumestrol antagonizes the S247W mutant significantly, regardless of whether rifampicin is present or which reporter system is used. Rifampicin does not significantly activate the S247W mutant, similar to data previously obtained (30). To simplify drug effects on PXR and exclude effects of drug on RXR binding or DNA binding, similar transcription assays were performed using a Gal4-PXR (one-hybrid) system (Fig. 5C). In this system, coumestrol antagonizes the S247W mutant significantly, whereas it has no effect

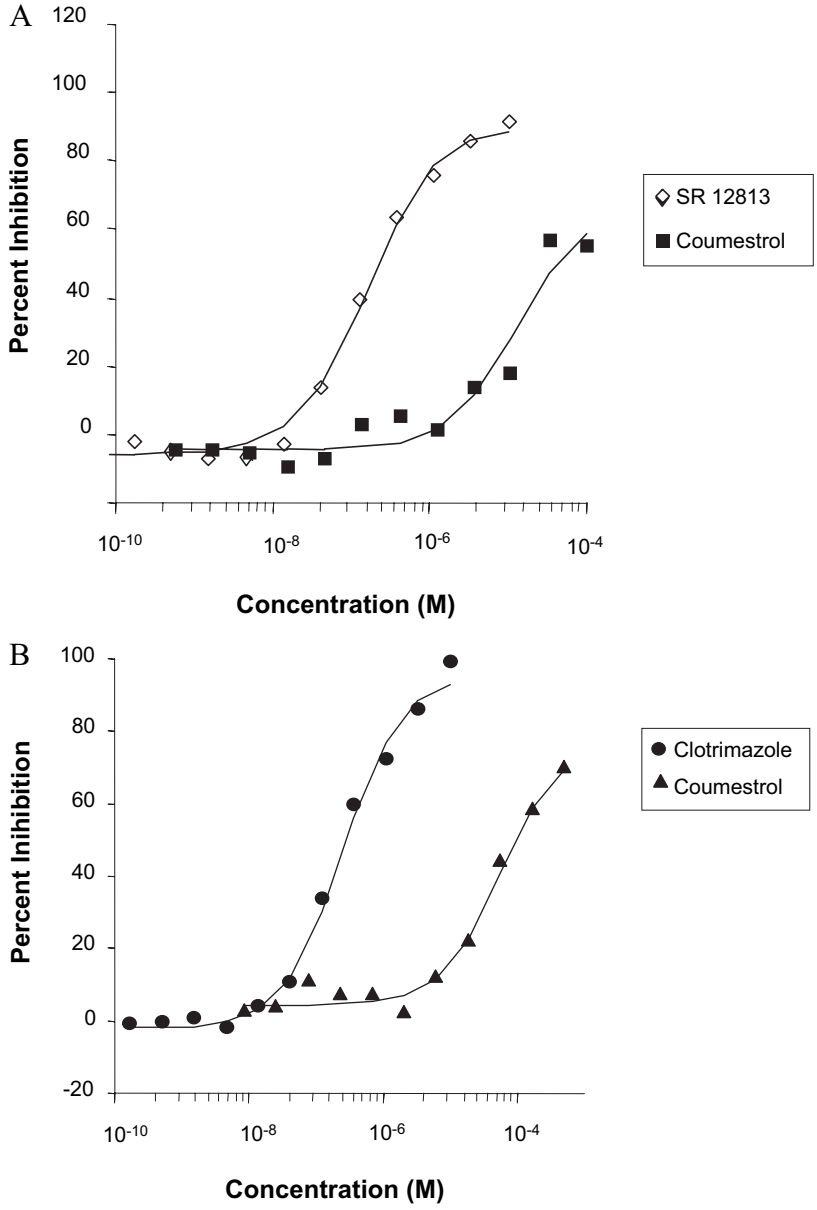

Fig. 4. Binding Assays

A, Purified human PXR bound to SPA beads was incubated in the presence of 10 nM PXR agonist [^{3}H]NMTB in the presence of increasing concentrations of unlabeled SR12813 (◇) or coumestrol (■). Displacement of [^{3}H]NMTB was measured in a Wallac Microbead counter. Data are expressed as a percentage of bound [^{3}H]NMTB in the absence of competitor. A K_i of 37 nM was observed for SR12813 and a K_i of 13 μM for coumestrol. B, Purified human CAR LBD bound to SPA beads was incubated with 10 nM [^{3}H]clotrimazole in the presence of increasing concentrations of unlabeled clotrimazole (●) or coumestrol (▲). A K_i of 250 nM was observed for clotrimazole, and a K_i of 54 μM was observed for coumestrol.

on Gal4-VP16 fusion protein-mediated transcription. Together, these data demonstrate that coumestrol antagonizes activated PXR even when a bulky residue obstructs its ligand-binding pocket. These data also suggest that coumestrol antagonizes PXR LBD because it has no effect on Gal4 binding, promoter binding, or RXR binding.

Because PXR has a promiscuous binding pocket, it is conceivable that even the S247W mutant can accommodate smaller ligands like coumestrol (MW 352.3) yet exclude larger ones like rifampicin (MW 822.9). To address this problem, we generated double and triple mutants of the PXR ligand-binding pocket in which the pocket is more filled with bulky residues. Combining that mutation with either S208W and/or C284W will effectively fill the ligand-binding pocket of PXR, leaving room insufficient to allow even the smallest established ligands (like SR12813 and estradiol) from binding to the receptor (9, 11) (also see Figs. 5F PXR mutant structure and 5F III). We show coumestrol

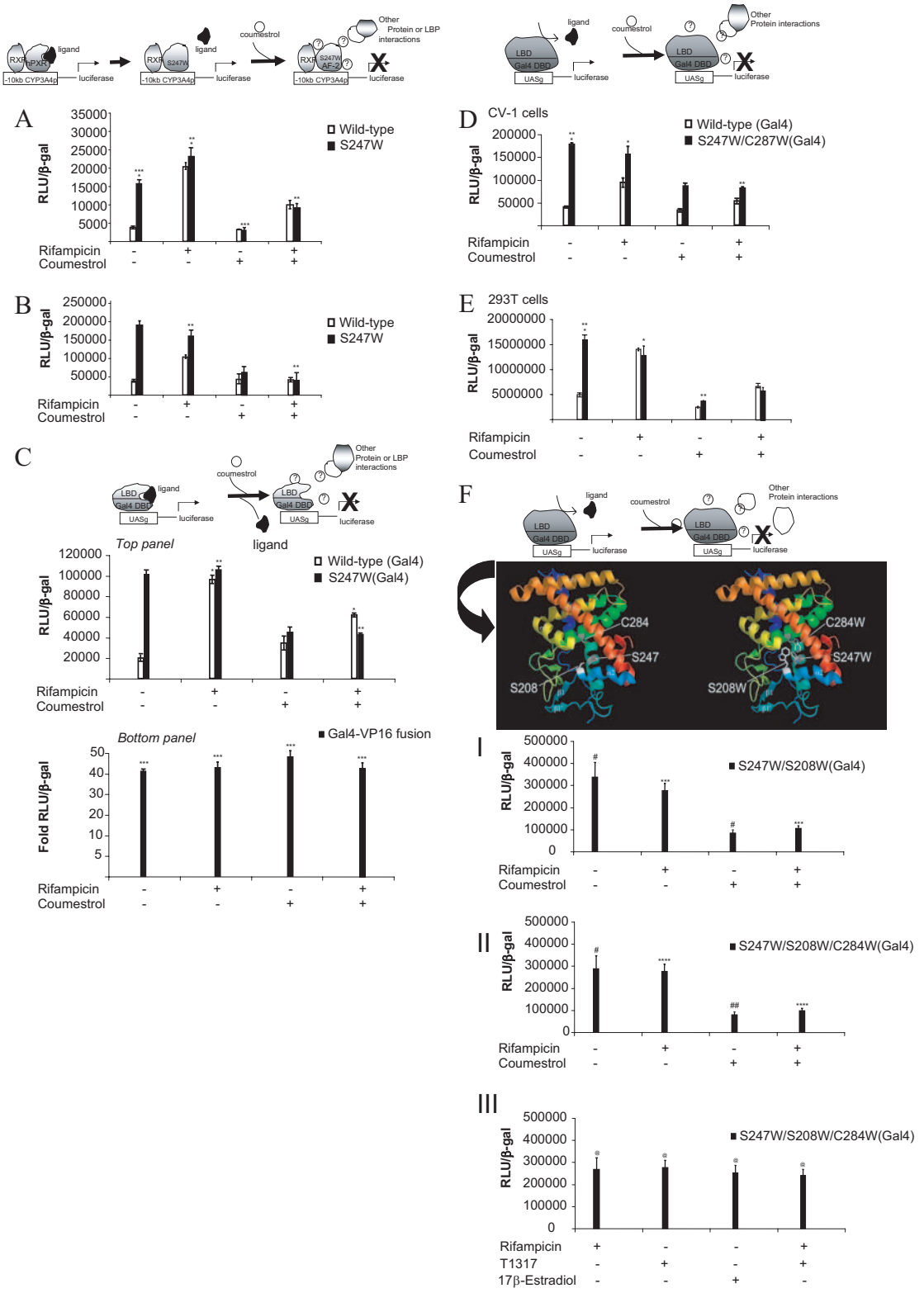

Fig. 5. Effect of Coumestrol on PXR Mutant Activity

A and B, CV-1 cells were transfected with expression plasmids for wild-type human PXR or PXR mutant (S247W) and the XREM-tk-Luciferase (A) or tk-MRP2-luc (B) reporter plasmid. Cell extracts were assayed for luciferase activity after compound treatment for 24 h. Drugs included rifampicin (10 μM) or coumestrol (25 μM) alone or in combination with rifampicin and/or T1317 (1 μM) or 17β-estradiol (20 μM). Data for each *column* represent the mean of two independent assays each performed in quadruplicate ± SE (*, $P > 0.8$; **, $P < 0.003$; ***, $P < 0.001$). LBP, Ligand-binding pocket. C and D, CV-1 cells were transfected with expression plasmids for Gal4-PXR or Gal4-PXR mutant (S247W) (C) or Gal4-VP16 fusion construct or Gal4-PXR double

significantly inhibits both double and triple mutants, which strongly suggests that PXR is antagonized by coumestrol at a site distinct from the ligand-binding pocket (Fig. 5, D–F).

To further understand the effects of coumestrol on PXR, we performed a ligand titration experiment with Gal4-PXR LBD using rifampicin (10–30 μM) in the presence or absence of a fixed concentration of coumestrol (25 μM). Although there is dose-dependent activation of Gal4-PXR in the presence of rifampicin, coumestrol antagonizes PXR activation to the same extent regardless of the concentration of rifampicin present (Fig. 6A). These data support the hypothesis that coumestrol binds and antagonizes PXR on its surface distinct from the ligand-binding pocket.

Mammalian Two-Hybrid Assays

To validate our findings from our transcription assays and to test the effects of coumestrol on the interaction of PXR and steroid receptor coactivator-1 (SRC-1), we performed mammalian two-hybrid assays using constructs and conditions for transfection as previously published (23). There is a ligand (rifampicin) dose-dependent interaction between PXR and SRC-1 (Fig. 6B). However, coumestrol antagonizes PXR and SRC-1 interactions to the same extent regardless of the ligand (rifampicin) concentration (Fig. 6B). In a separate set of experiments, rifampicin increases the association of full-length human PXR and SRC-1 in cells nearly 4-fold. Coumestrol alone has no significant effect on the association of PXR and SRC-1; however, in the presence of rifampicin, coumestrol significantly disrupts the association of PXR and SRC-1 by a magnitude of 3.2-fold. By contrast, in the presence of rifampicin, coumestrol diacetate increases the association of human PXR with SRC-1. T1317, another potent human PXR agonist, increases the association of PXR and SRC-1. As shown for rifampicin, coumestrol significantly antagonizes the T1317-mediated association of PXR and SRC-1 (Fig. 7A). To determine whether the N-terminal region of human PXR (excluding the LBD) is important or required for coumestrol action, we repeated the mammalian two-hybrid assays this time using only the LBD of PXR fused to activation domain VP16 as prey. In this assay, in the presence of rifampicin, coumestrol significantly disrupts the association of PXR and SRC-1 by a magnitude of 3.1-fold (Fig. 7B). These results are nearly identical to that observed for full-length PXR, demonstrating that the N terminus of PXR is not required or important for coumestrol action. Taken together, these data indicate that coumestrol acts as a PXR antagonist by disrupting coregulator-specific interactions within the LBD of the receptor but with at least one inhibitory site outside the ligand-binding pocket.

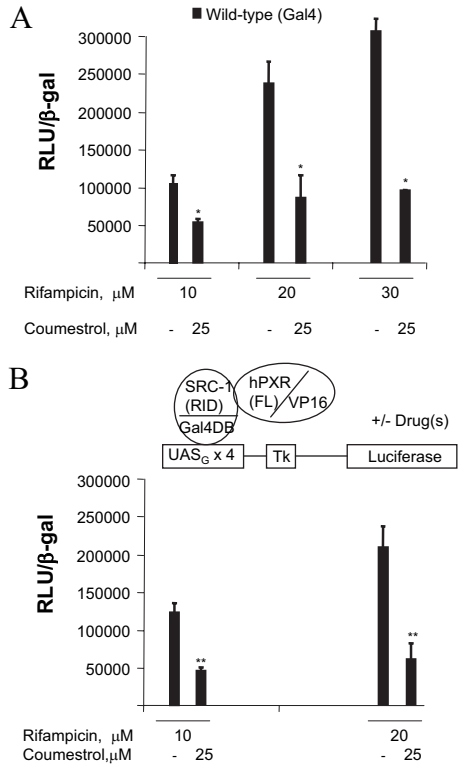

Fig. 6. Effect of Coumestrol on PXR-Mediated Transcription and Binding of Coactivator SRC-1 with PXR

CV-1 cells were cotransfected with expression plasmids for human PXR and the XREM-tk-Luciferase reporter vector (A) or human FL PXR-VP16 plasmid (B) and Gal4-SRC-1 receptor interacting domain (RID), and UASg-Tk-luc reporter. Cell extracts were assayed for luciferase activity after compound treatment for 24 h. Cell extracts were assayed for luciferase activity after drug treatment for 48 h. Drugs included rifampicin (10–30 μM) and coumestrol (25 μM). Data for each *column* represent the mean of three independent assays performed in triplicate ± SE. *, $P > 0.1$; **, $P > 0.3$.

mutant (S247W/C287W) (D) and treated with drug(s) as shown. E, The identical experiments as shown in D were performed in HEK293T cells. C, *Top panel*, Data for each *column* represent the mean of two independent assays each performed in triplicate ± SE (*, $P < 0.001$; **, $P < 0.0001$); *bottom panel*, data for each *column* represent the mean of three independent assays each performed in triplicate ± SE (***, $P > 0.2$). F, Same experiment as described in D. The PXR expression plasmid is Gal4-PXR (I) double mutant (S247W/S208W) or (II, III) triple mutant (S247W/S208W/C284W). D–F, Data for each *column* represent the mean of three independent assays each performed in triplicate ± SE (*, $P > 0.1$;**, $P < 0.0001$; #, $P < 0.002$; ***, $P < 0.01$; ****, $P < 0.003$; ##, $P < 0.002$; @, $P > 0.3$). *Illustration* in F, S247W is a mutation that is known to lead to ligand-independent activation of PXR (30). It also fills a significant portion of the ligand-binding pocket of the receptor. Combining that mutation with either S208W or C284W will effectively fill the ligand-binding pocket of PXR, leaving room insufficient to allow even the smallest established ligands (like SR12813) from binding to the receptor.

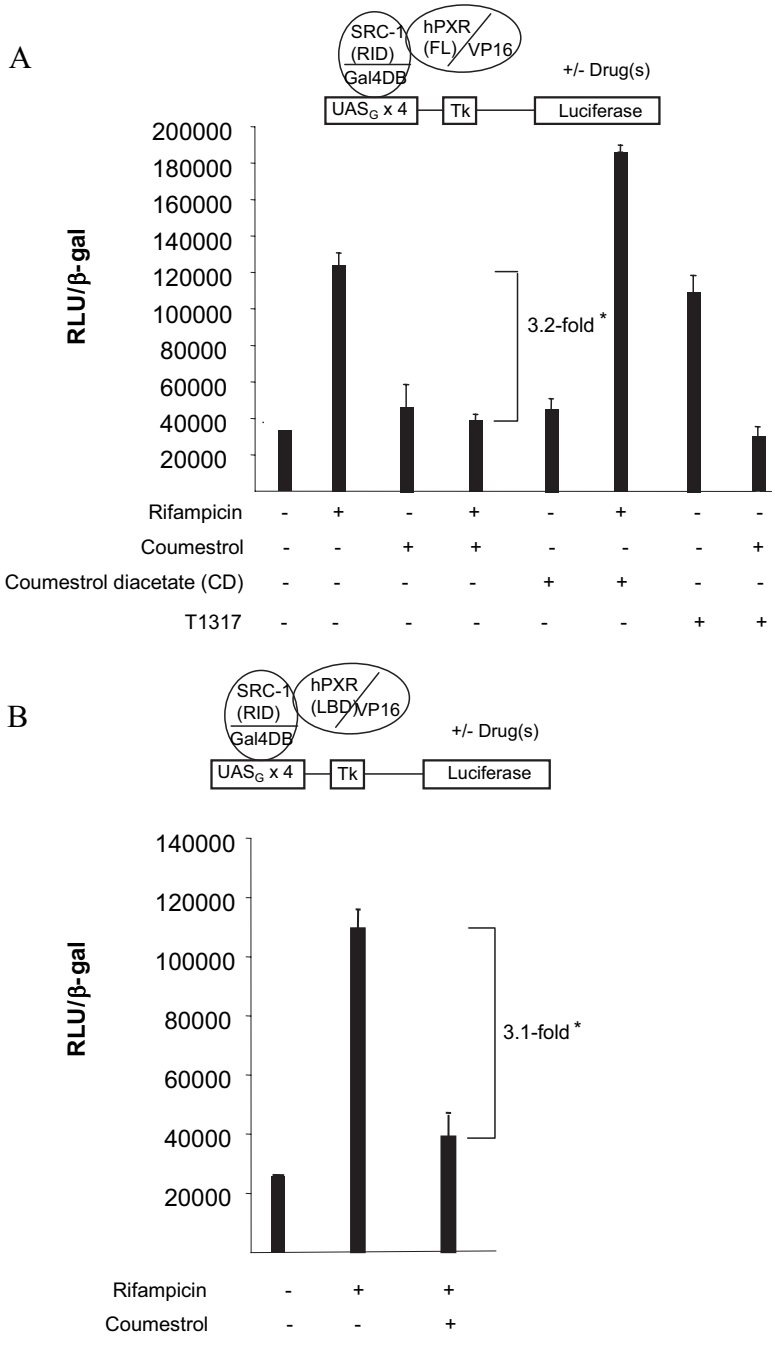

Fig. 7. Effect of Coumestrol on Binding of Coactivator SRC-1 with PXR

Mammalian two-hybrid assays were performed in HEK293T cells to study the interaction of human PXR with SRC-1 in the presence or absence of drug(s). The cells were transfected with human FL PXR-VP16 plasmid (A) or human LBD PXR-VP16 plasmid (B) and Gal4-SRC-1 receptor interacting domain (RID), and UASg-Tk-luc reporter. Cell extracts were assayed for luciferase activity after drug treatment for 48 h. Drugs included rifampicin (10 μM), coumestrol, and coumestrol diacetate (25 μM each). Data for each *column* represent the mean of two independent assays performed in triplicate $\pm$ SE. *, $P < 0.05$.

Fluorescence Polarization (FP) Competition Assays

To address whether the binding of coumestrol to the surface AF-2 site of PXR could be observed *in vitro*, we conducted the following competition assay. The displacement of an Flc-labeled SRC-1 LxxLL-containing peptide from the AF-2 surface of the PXR LBD with increasing concentrations of coumestrol was monitored using FP methods. Because the peptide is displaced from its binding site on the LBD, its FP decreases. These experiments were performed with

either coumestrol, which is expected to bind to the PXR AF-2 site, or coumestrol diacetate, which is not expected to bind to the same site. Low coumestrol and coumestrol diacetate solubility made these experiments difficult, despite the fact that 25% dimethylsulfoxide (DMSO) was employed. Dilutions of these putative antagonists made in the buffer necessary to do the assay lead to precipitation of ligand only (no protein was detected in these insoluble fractions by SDS-PAGE). Thus, the antagonist solutions were filtered to remove insoluble aggregates, and both the unfiltered and filtered solutions were employed. Thus, the studies were conducted to determine whether coumestrol was simply capable of dissociating an LxxLL-containing coactivator motif more effectively than coumestrol diacetate.

The EC_{50} range of unfiltered coumestrol was calculated to be 1.2–1.3 mM ($R^2 = 0.985$); from the EC_{50} value, the coumestrol K_i range was calculated to be 1.2–1.3 mM. It is theorized that this value is high due to the coumestrol that precipitated out of solution. The same experiment performed with coumestrol diacetate yielded curves indicating a weaker ability to dissociate the labeled LxxLL peptide, as expected. The curves for the filtered solution show the same trend, no dissociation of the peptide with coumestrol diacetate but some dissociation with coumestrol. Taken together, these data support the conclusion that coumestrol specifically disrupts coactivator binding to the surface of PXR.

Effects of Coumestrol on PXR Localization in Wild-Type and Humanized PXR Mice

In wild-type mice, the subcellular localization of PXR has been shown to be the cytoplasm as visualized using a primary antibody directed against mouse PXR. PCN treatment results in recruitment of PXR to the nucleus. These results are identical to those observed and reported previously (31). Coumestrol has no significant effect on basal staining using a PXR antibody and, furthermore, does not disrupt the nuclear pattern of staining observed in the presence of PCN (Fig. 8). Similarly, we stained livers from humanized PXR mice, and the basal staining for PXR was predominantly nuclear. However, the intensity of staining increased markedly in the presence of rifampicin. Coumestrol has no significant effect on either basal or rifampicin-

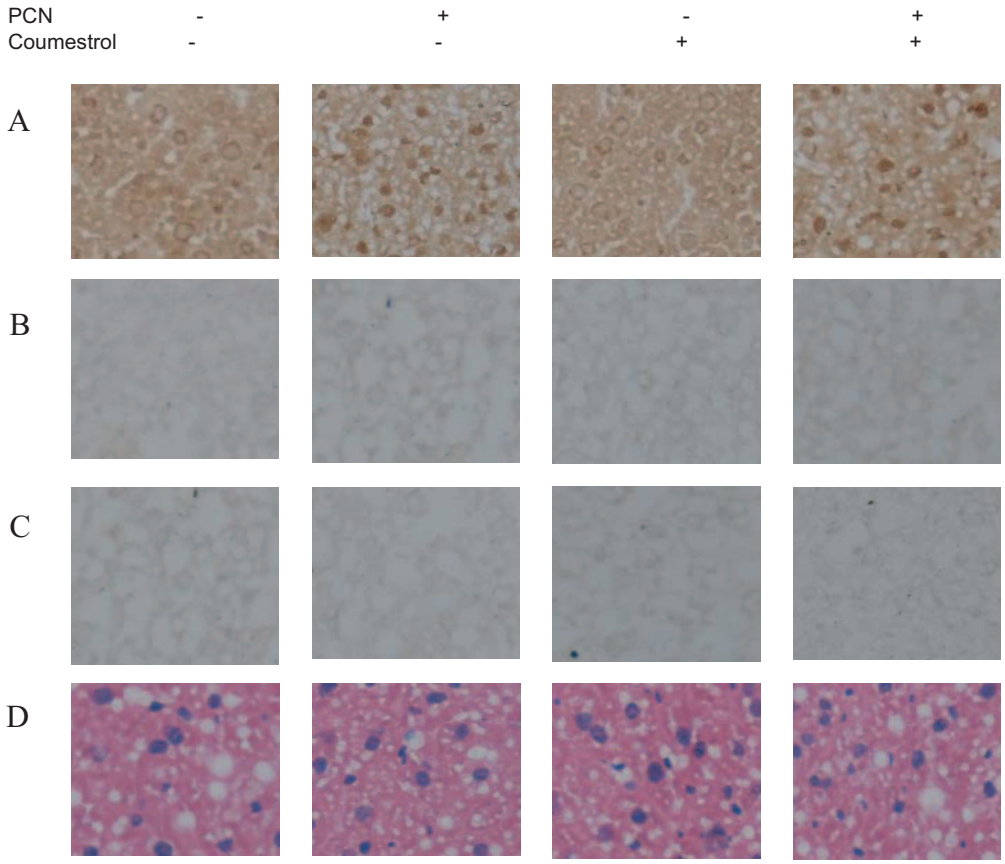

Fig. 8. Effect of Coumestrol on Subnuclear Localization of PXR in Wild-Type Mouse Liver

The photomicrographs show the effect of drug(s) on mouse liver tissue expressing PXR. Three mice from each treatment group were killed after completing LORR studies (see *Materials and Methods* and Fig. 12). A, Liver tissue was immunoassayed for PXR. The remaining panels show controls: B, no primary antibody; C, PXR protein; D, H&E stain. Fifteen sections of each liver were made and stained. The picture is the best representative section of all stained slides.

induced staining for PXR (Fig. 9). Together, these results suggest that coumestrol does not alter PXR localization. To determine the localization of PXR and effects of coumestrol on transfected PXR, we performed cellular localization studies with green fluorescent protein (GFP)-tagged human PXR. On transfection of GFP-PXR, the fluorescent signal is largely localized within the nucleus. Addition of rifampicin causes granular deposits (speckled appearing, ~34% of nuclei) within the nucleus (Fig. 10B). Similarly, the intensity of speckling and amount of speckled nuclei increases significantly with cotransfection of SRC-1 plasmid (~63% of nuclei) (Fig. 10E). These results corroborate previous findings using the same constructs (32). Coumestrol has no effect on basal speckling (~8 *vs.* 11% of nuclei, $P > 0.2$; Fig. 10). Importantly, coumestrol has no effect on rifampicin-induced granularity (speckle-appearing bodies) (34 *vs.* 39% of nuclei, $P > 0.1$; Fig. 10). By contrast, coumestrol significantly inhibits the bright speckling pattern observed with rifampicin (63 *vs.* 24% of nuclei, $P < 0.001$). The pattern of speckling in GFP-PXR and SRC-1 cotransfected cells treated with rifampcin and coumestrol is nearly identical to that observed for GFP-PXR transfected cells (compared Fig. 10, E *vs.* B). These results suggest that coumestrol does not alter either the basal or rifampicin-induced localization of human PXR. On the contrary, these results support coumestrol's effect as an inhibitor of PXR and SRC-1 interaction.

Effects of Coumestrol on Gene Expression in Primary Human Hepatocytes

Based on the finding that coumestrol reduces PXR activity in *in vitro* and cell-based assays, we next tested whether this activity would be reflected in cellular effects on gene expression. PXR has been shown to regulate genes involved in xenobiotic detoxification (2, 8) including *CYP3A4* and *CYP2B6*. The effects of coadministration of two established PXR agonists (SR12813 and rifampicin) with coumestrol were assessed in primary human hepatocytes. SR12813 was dosed at 1 μM and rifamipicin at 10 μM, both at approximately 10-fold their respective EC_{50} values in PXR transient transfection assays. Coumestrol was used at a concentration of 25 μM, a concentration of coumestrol consistent with those used in other studies (33).

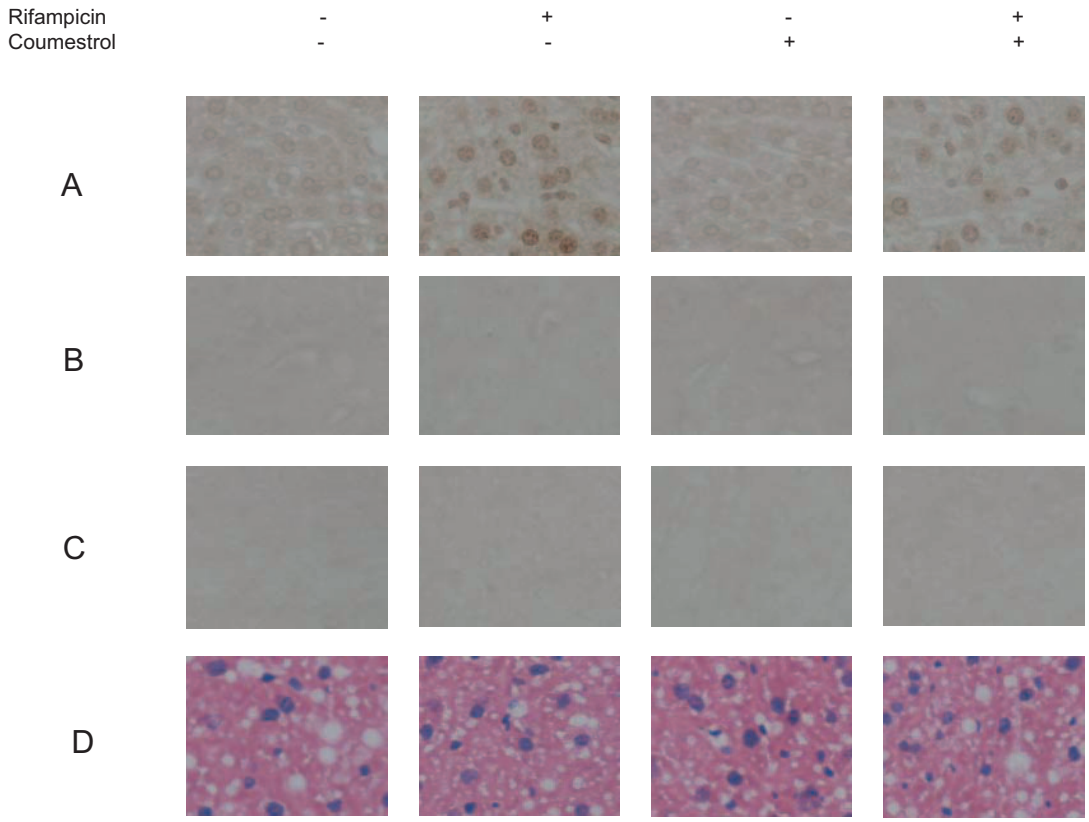

Fig. 9. Effect of Coumestrol on Subnuclear Localization of PXR in Humanized Mouse Liver

The photomicrographs show the effect of drug(s) on mouse liver tissue expressing human PXR. The same numbers of mice as in Fig. 8 were killed. A, Liver tissue was immunoassayed for human PXR. The remaining panels show controls: B, no primary antibody; C, PXR protein; D, H&E stain. Fifteen sections of each liver were made and stained. The picture is the best representative section of all stained slides.

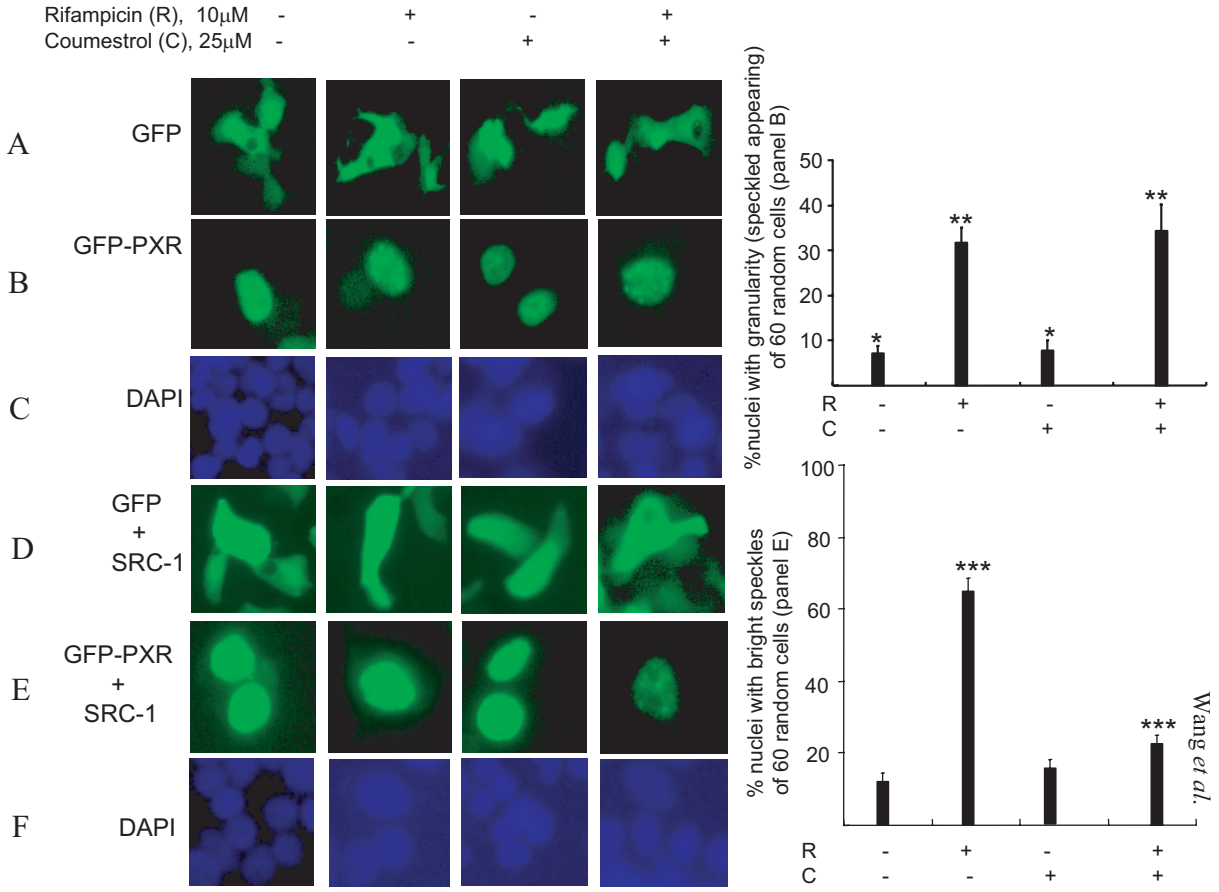

Fig. 10. Effect of Coumestrol on Subnuclear Localization of PXR

The photomicrographs show the effect of drug(s) on HEK293T cells expressing GFP (A) or GFP full-length human PXR (B) and/or SRC-1 (D and E). Twenty-four hours after transfection, 293T cells were treated with vehicle (0.2% DMSO), rifampicin (R) 10 μM, coumestrol (C) 25 μM, or both drugs for 4 h in serum-free media. The cells were fixed with 10% paraformaldehyde for 20 min and then mounted using mounting medium containing 4′,6-diamidino-2-phenylindole stain. The cells were imaged by confocal microscopy at ×40 magnification using the appropriate fluorescent channels. For quantification of granular or bright speckled nuclei (B and E, respectively), 60 cells (about four to five cells per high-power field scanning a total of 15 fields) were randomly counted for each experiment, and a representative picture from three independent experiments is shown. *, $P > 0.2$; **, $P > 0.1$; ***, $P < 0.001$.

Quantitative changes in *CYP3A4* expression was assessed in primary human hepatocytes (two donors) by Northern blot analysis and expressed as fold changes relative to vehicle controls (Fig. 11, A and B). Coumestrol was able to block the induction of *CYP3A4* by PXR agonists in both donors (Fig. 11, A and B). In donor 1, basal *CYP3A4* mRNA steady-state levels were undetectable, and treatment with coumestrol alone did not increase the basal level of *CYP3A4* mRNA to detectable levels. Both rifampicin and SR12813 treatment resulted in induction of *CYP3A4* mRNA (the SR12813 treatment induced *CYP3A4* to approximately 20% of the levels induced by rifampicin). Rifampicin-mediated induction of *CYP3A4* was decreased by approximately 50% by 25 μM coumestrol, and the induction by SR12813 was completely abolished by cotreatment with 25 μM coumestrol. Thus, coumestrol was able to block the activation of both rifampicin and SR12813 of *CYP3A4* expression in primary human hepatocytes. Similar results were obtained in a second donor (Fig. 11B), except in this donor, the basal level of *CYP3A4* gene activity was higher. Again, coumestrol did not increase the basal activity and partially blocked the effects of PXR agonists rifampicin and SR12813 when coadministered. The induction of target genes by the PXR agonists in donor 1 was much more dramatic than in donor 2. Such inter-donor variation is not without precedent, and it is well established that *CYP3A* expression is quite variable in human primary hepatocyte preparations (34, 35). The differences in the relative magnitude of induction between donors are likely a reflection of differences in basal levels of expression of target genes. The normal high level of interindividual variation would be expected to be magnified in sets of hepatocytes obtained by human donors typically undergoing drug therapy and hospitalization.

The effects of coumestrol on *CYP2B6* expression were generally analogous to the *CYP3A4* results.

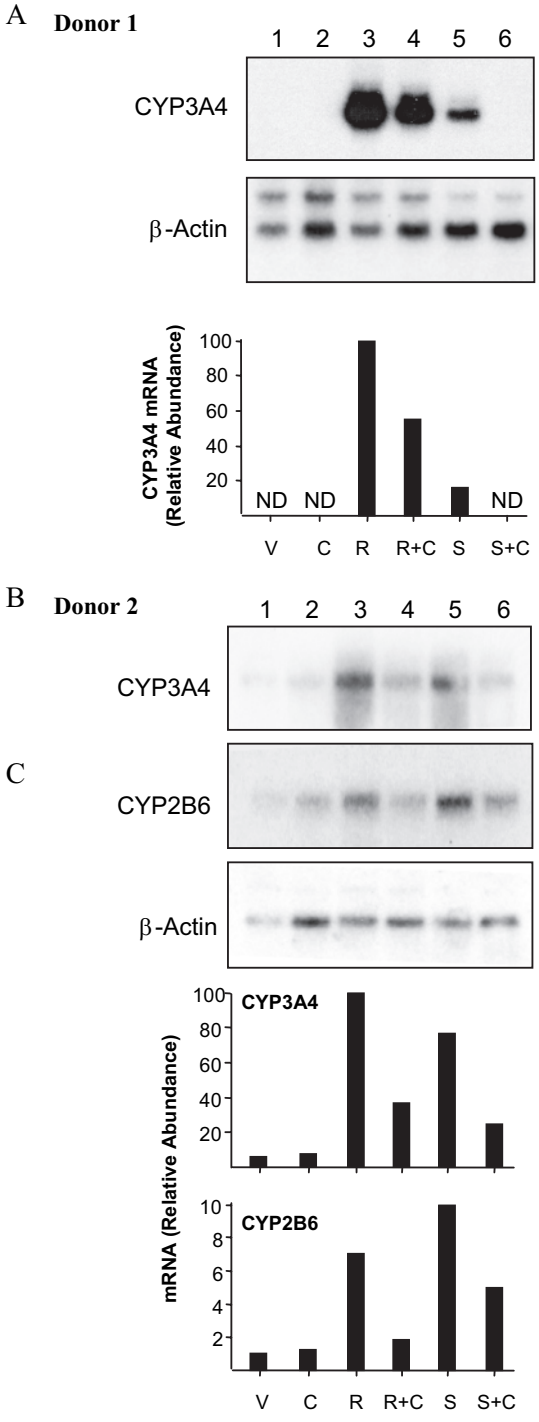

Fig. 11. Effects of Coumestrol on *CYP3A4* and *CYP2B6* Expression

Total mRNA was isolated from two donors of primary human hepatocytes and treated with vehicle (V, DMSO), coumestrol (C, 25 μM), rifampicin (R10 μM), coumestrol plus rifampicin (R+C, 25 and 10 μM, respectively), SR12813 (S, 1 μM), and coumestrol plus SR12813 (S+C, 25 and 1 μM, respectively). After Northern blotting, the RNAs from were probed with a fragment of the human *CYP3A4* coding region (donors 1 and 2) or *CYP2B6* (donor 2) and visualized by autoradiography. Relative mRNA abundance (normalized for β-actin mRNA levels) is plotted below each autoradiogram.

Northern blot analysis (one donor) showed that rifampicin and SR12813 were effective at inducing *CYP2B6* in donor 2 (Fig. 11C). Cotreatment with coumestrol reduced the level of induction of both of the PXR agonists. The 7-fold *CYP2B6* induction by rifampicin was reduced to 2-fold in the presence of coumestrol, and the 10-fold induction by SR12813 was reduced to 5-fold by coadministered coumestrol. In summary, coumestrol affected a pattern of expression in primary hepatocytes that were consistent with PXR antagonism and could not be predicted from effects of coumestrol on the ER.

Loss of Righting Reflex (LORR) Studies in *PXR* (+/+), Humanized PXR, and *PXR* (−/−) Mice

In vivo effects of coumestrol on drug metabolism was assessed using mice with or without functional *PXR* gene. In these assays, the consequences of activating *PXR* can be studied using mice challenged with 2,2,2-tribromoethanol (Avertin) anesthesia, where the drug-induced change in duration of LORR acts as a phenotypic measure of *PXR* target gene activity and xenobiotic metabolism (18, 23). PCN significantly decreases tribromoethanolamine-induced sleep time or duration of LORR in *PXR* (+/+) mice. Coumestrol has negligible effects on the duration of LORR in these mice. Furthermore, in the presence of a PXR agonist (PCN), coumestrol does not significantly increase the LORR duration (1.0 $\pm$ 0.7 *vs.* 2.4 $\pm$ 0.8 min, $P > 0.1$). Similarly, in the presence of PCN, coumestrol diacetate does not increase the duration of LORR. In mice lacking the *PXR* allele, there is no effect of PCN, coumestrol, or coumestrol diacetate on the duration of LORR when compared with that observed in control mice. In mice carrying the human *PXR* allele, coumestrol significantly increases the rifampicin-mediated duration of LORR by 173% ($P < 0.001$) (Fig. 12).

DISCUSSION

We have shown that coumestrol is a human PXR and CAR antagonist in *in vitro* assays and that this naturally occurring phytoestrogen can block the effects of an available PXR agonist in primary human hepatocyte cultures. Coumestrol does not affect the localization of PXR when it is activated by its cognate ligand. These results suggest that coumestrol acts directly on PXR and/or its coregulatory proteins and/or promoter interactions. Further support of this conclusion comes from published studies that demonstrate coumestrol regulates intracellular receptors (*e.g.* ERα) and kinases [*e.g.* MAPK kinase 1 kinase (MEK1), phosphatidylinositol 3-kinase (PI3K)] that in turn have been shown to phosphorylate key coregulators [*e.g.* SRC-1, silencing mediator for retinoid and thyroid receptors, forkhead (transcription factor) box O1] that activate PXR (36–41). Hence, the cellular effects of coumestrol should activate PXR; however, we show

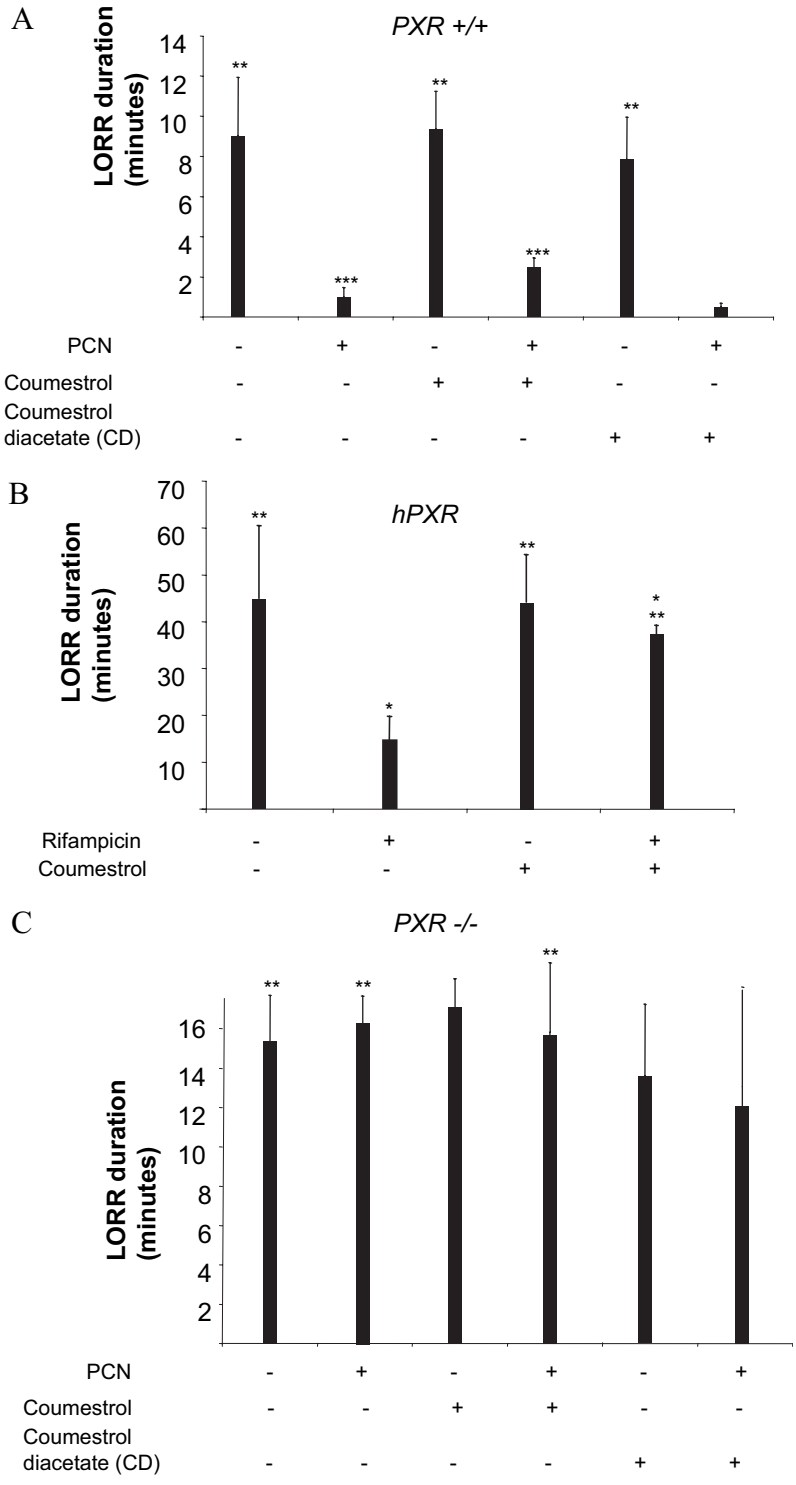

Fig. 12. Effect of Coumestrol and Its Analogs on Anesthetic (Tribromoethanolamine) Metabolism *in Vivo*

A and B, LORR duration assessments to determine the effect of coumestrol and its analogs, diacetate and dimethyl ether, in *PXR (+/+)* (A) and *PXR (−/−)* (B) mice. Six- to 8-wk-old C57BL/6 female mice (n = 5 per treatment group) were treated with vehicle or PCN or coumestrol, coumestrol diacetate, or the combination of PCN plus coumestrol or its analog (see *Materials and Methods* for details). On d 6, all mice underwent LORR duration assessments as described previously (23). *Columns* represent the mean and *error bars* ± SE. *, $P < 0.001$; **, $P > 0.3$; ***, $P > 0.1$.

inhibition of PXR activity and PXR target genes. This further supports our hypothesis that coumestrol must have overriding functions upon direct interaction with PXR and/or its coregulators.

The scintillation proximity assay (SPA) results demonstrate that in the concentrations used for the transcription assays, coumestrol can act as a competitive inhibitor for ligand binding in the PXR ligand-binding pocket. In support of these findings, yeast and mammalian two-hybrid assays (for yeast two-hybrid assays, see supplemental Fig. 1S, published as supplemental data on The Endocrine Society's Journals Online web site at http://mend.endojournals.org) and S247W transcription assays together show that coumestrol inhibits PXR (*e.g.* either within the ligand-binding pocket or outside or both). From the mammalian two-hybrid experiments with full-length and PXR LBD plasmids, it is clear that the N-terminal domain of PXR is not important for coumestrol effects on the receptor. However, pocket-filling (obliterating) mutants of PXR are still inhibited by coumestrol, suggesting that in addition to binding to the pocket, coumestrol binds to a surface outside the pocket. To further corroborate this hypothesis, we show that coumestrol inhibits PXR and SRC-1 interactions to the same extent regardless of the concentration of agonist ligand present. Together, in addition to ligand competition effects, these data suggest that coumestrol inhibits PXR by binding to additional surface site(s) outside the pocket (*e.g.* AF-2 region). Modeling studies cannot currently predict exactly why coumestrol is acting as an antagonist. It will be necessary to solve the crystal structure of the coumestrol-PXR complex or carry out functional studies combined with site-directed mutagenesis to define key LBD or AF-2 residues that interact with coumestrol.

We performed *in vitro* experiments to examine the impact of coumestrol on SRC-1 binding to PXR using FP anisotropy assays (see supplemental Fig. 2S). We showed a weak disruptive effect of coumestrol on the binding of fluorescently labeled SRC-1 to the AF-2 site on purified PXR LBD in the presence of SR12813. The effect with coumestrol diacetate was weaker in the same assay by 10-fold. These assays were difficult to conduct due to the incompatible solubility of the coumestrol compounds and the PXR LBD in the same buffer conditions. However, the results we obtained support the conclusion that coumestrol, but not coumestrol diacetate, disrupts the association of PXR for the coactivator SRC-1.

Despite these results, there is support for the discordance between *in vitro* binding assay and transcription-based assays. Zhu *et al.* (42) notes that although there is good correlation between results of transactivation and binding assays, there are several compounds where discrepancies are noted (*e.g.* high binding affinity in binding assays translate to low transactivation). These experiments and data underscore the importance of performing both transcription as well as *in vitro* protein binding assays to determine the mechanisms that are likely involved in the inhibitory action of drugs on nuclear receptors (16).

Coumestrol is the second plant-derived compound shown to affect PXR activity. PXR has previously been shown to mediate the effects of the botanical hyperforin (an active component of the herb St. John's wort) on induction of *CYP3A4* activity (43), which is associated with clinically significant drug interactions (44, 45). In some instances, these interactions were life-threatening or lethal (46, 47).

Our finding that coumestrol is a PXR antagonist is a surprising result given that coumestrol has previously been reported to act as a PXR (also known as SXR) agonist in transient transfection assays (48). In those studies, a different promoter was used in the reporter construct (a multimerized DR4 element). When we repeated our transient transfection studies using a reporter construct containing the same multimerized DR4 promoter, coumestrol profiled as a PXR antagonist with the same potency seen on the XREM reporter (data not shown). We cannot account for this difference in coumestrol activity between the two reports. We used coumestrol in our experiments immediately after solubilization in solvent. Because coumestrol is chemically labile (*e.g.* is insoluble in cold water, is liable to degradation during long-term storage, and may form conjugates in acidic conditions like the isoflavones) (49), it is also possible that differences in chemical storage resulted in unknown breakdown products with PXR agonist activity in the earlier report. As we have shown above, two coumestrol analogs are not active as antagonists but are weak agonists (see Fig. 2). In transfections using human PXR, coumestrol significantly inhibits rifampicin-activated PXR (see Fig. 2B); however, coumestrol diacetate and dimethyl ether do not alter the activation of PXR in the presence of rifampicin (Fig. 2B).

Dramatic interspecies differences in activation of PXR orthologs has been well documented (26). We tested coumestrol in full dose-response curves in transient transfection using mouse PXR, and coumestrol did not significantly suppress (or activate) mouse PXR ($EC_{50} > 50$ μM, supplemental Fig. 3S). This species difference may be useful in defining key regions of the LBD involved in the coumestrol antagonist effects. The results from our *in vitro* transcription assay using one concentration point of coumestrol was validated in mice carrying PXR (+/+) allele where the LORR duration was not significantly altered by coumestrol in the presence of PCN (Figs. 2A and 12). Together, in contrast to the inhibitory effect of coumestrol on human PXR, there is no significant effect of the compound on mouse PXR.

Coumestrol diacetate can potentially be converted to coumestrol by cleavage of the acetate groups by cellular esterases. To test whether there could be a potential for conversion and hence true effects of the diacetate analog being masked by cellular conversion to coumestrol, we performed transient transcription assays identical to those done and results shown in Fig. 2. In the same cell line, we first used two different concentrations of coumestrol diacetate (25 and 75 μM) for 48 h before cell lysates were analyzed and normalized for lucif-

erase activity. The relative light units/β-galactosidase (β-gal) values were nearly identical for both concentrations of coumestrol diacetate in the presence of 10 μM PCN [$P > 0.2$, supplemental Fig. 4S(A)]. Furthermore, we repeated the same experiment but with two different concentrations of coumestrol diacetate (5 and 25 μM) for 72 h before cell lysates were analyzed and normalized for luciferase activity. In these experiments, the relative light units/β-gal values for both concentrations of coumestrol diacetate were also nearly identical in the presence of 10 μM PCN [$P > 0.3$; experiment was performed twice each in quadruplicate, supplemental Fig. 4S(B)]. Both sets of experiments were designed to test the hypothesis that time- and concentration-dependent conversion of coumestrol diacetate to coumestrol could result in changes in intracellular coumestrol and be reflected in significant changes in human PXR activity. In particular, longer exposure (2-fold increase in duration of exposure) and higher concentrations (3-fold increase in concentration) of the diacetate analog would result in greater amounts of coumestrol within cells. These levels might then inhibit human PXR activity. We did not observe any significant effect on human PXR activity. These results suggest that it is unlikely that there is significant conversion of coumestrol diacetate to coumestrol in cells. Lesser amounts of conversion does not significantly affect the effect of coumestrol diacetate on PXR activity. These results are further corroborated in experiments where coumestrol diacetate was incubated in CV-1 cell extract. Mass spectrometry did not reveal any conversion to coumestrol (supplemental Fig. 5S). The hydroxyl ring in the 3,9-position of coumestrol is altered to diacetate or dimethyl ether groups, and these analogs do not exhibit the inhibitory activity on PXR as its parent 3,9-dihydroxy compound. Together, this suggests that both hydroxyl groups on the benzyl rings are critical for PXR activity.

In summary, coumestrol provides a commercially available and chemically simple antagonist tool for PXR structure/function studies. Multiple compounds with structural similarity to coumestrol could be screened to find additional and possibly more potent tools for PXR structure function analysis. Overall, these studies may provide additional insight into mechanisms of PXR activation while suggesting new avenues of PXR antagonism to prevent harmful drug-drug interactions and improving therapeutic efficacy.

MATERIALS AND METHODS

Chemicals

Coumestrol was purchased from Fluka (Milwaukee, WI), 98% pure via thin-layer chromatography (MW 268.2). Coumestrol diacetate (7,12-diacetoxycoumestan *O*,*O*′-diacetylcoumestrol, MW 352.3) and coumestrol dimethyl ether (7,12-dimethoxycoumestan, MW 296.3) were purchased from Fluka (≥95% pure via HPLC). 17β-Estradiol was purchased from Sigma-Aldrich (St. Louis, MO), and T1317 was supplied by GlaxoSmithKline (Dr. J. Collins, Research Triangle Park, Durham, NC). The compound was freshly prepared by dissolving in DMSO before each use.

Cotransfection Assays

CV-1 cells were maintained and transiently transfected essentially as previously described (50). Receptor constructs contained coding sequences for AR (NR3C4), PR (NR3C3), GR (NR3C1), ERα and -β (NR3A1/3A2), MR (NR3C2), RARα (NR1B1), PXR (NR1I2), CAR (NR1I3), RXRα (NR2B1), TRα and -β (NR1A1/1A2), VDR (NR1I1), FXR (NR1H4), LXRα and -β (NR1H3/1H2), and PPARα, -γ, and -δ (NR1C1/1C2/1C3). The following receptors were transfected as Gal4-LBD chimera constructs (PPARα, PPARδ, PPARγ, RARα, VDR, TRα, TRβ, LXRα, LXRβ, and FXR) in combination with a UAS-tk-luciferase reporter. In the transfections using PXR, GFP-PXR, LXRα, LXRβ, and FXR constructs, an expression plasmid encoding the coactivator SRC-1 was included as described previously (26, 32). The remaining receptors (GR, PAR, AR, MR, RXRα, PXR, CAR, ERα, and ERβ) were tested using full-length receptor expression constructs. The reporters used were pLM253-MMTV-Luciferase for GR, PAR, AR, and MR (51), pCRBPII-tk-SPAP for RXRα (52), XREM-luciferase for PXR and CAR (53), −10-kb CYP3A4-luciferase (Dr. Jonas Uppenberg, Stockholm, Sweden) and tk-MRP2-luc (Dr. Wen Xie, University of Pittsburgh, Pittsburgh, PA) for PXR, and 2xERE-tk-SPAP for ERα and ERβ (54). The ERα and ERβ assays were run in T47D cells instead of CV-1. The mammalian two-hybrid assays were performed (for PXR) using gal4 SRC-1 chimera (Dr. Akira Takeshita, Tokyo, Japan) and full-length human (FL) or LBD PXR-VP16 chimera (Drs. Bruce Blumberg and Ronald M. Evans, University of California-Irvine, Irvine, CA) in HEK293T cells as previously described (18, 23).

Site-specific mutations were made using the QuikChange-II Site-Directed Mutagenesis Kit (Stratagene, La Jolla, CA) protocol for PCR using manufacturer guidelines. The following primers were used (*underlining* indicate mutated nucleotides): S247W primers, forward 5′-gctgacatg*TGG*acctacatgttc-3′ and reverse 5′-gaacatgtaggt*CCA*catgtcagc-3′; S208W primers, forward 5′-aaagatctgtgc*TGG*ttgaaggtctct-3′ and reverse 5′-agagaccttcaa*CCA*gcacagatcttt-3′; and C284W primers, forward 5′-gctttcgagctg*TGG*caactgagattc-3′ and reverse 5′-gaatctcagttg*CCA*cagctcgaaagc-3′.

The mutations were generated using pM-Gal4-PXR-LBD plasmid as template sequentially to generate the S247W and S247W/S208W, S247W/C284W, and S247W/S208W/C284W LBD mutants. XL-blue competent cells were used to transform the PCR products (981 bp), and bacterial colonies were used to isolate plasmid DNA. All clones were sequenced to confirm and verify mutations.

Yeast Two-Hybrid Assays: Bacterial and Yeast Strains

Yeast strain CTY10–5d (*MATa ade2 trp1-901 leu2-3*, *I12his3-200 gal4*$^-$ *gal80*$^-$ *URA3*::*lexA-lacZ*) contains an integrated GAL1-lacZ gene with lexA operator and was kindly provided by Dr. G. V. Kalpana, Albert Einstein College of Medicine, Bronx, NY. Transformation of yeast and qualitative 5-bromo-4-chloro-3-indolyl β-D-galactosidase (X-Gal) nitrocellulose filter lift assays were performed according to published methods with minor modifications (55–57). Quantification of protein-protein interactions was determined using a β-gal liquid assay, which was performed on permeabilized yeast grown from three independent transformants using orthonitrophenyl-β-D-galactopyranoside as substrate (Clontech Laboratories, Inc., Palo Alto, CA; protocol PT3024-1; version

PR13103). *Escherichia coli* strain DH5α (Bethesda Research Laboratories, Bethesda, MD) was used for cloning plasmids.

Construction of PXR and SRC-1 Fusions in Yeast Vectors

Yeast vectors pGAD2f (gift from Dr. Stan Fields, State University of New York, Stony Brook, NY), pSH2-1 (58), and pGADNot (59) were used for cloning bait and prey. Briefly, human PXR LBD (amino acids 107–434) was PCR amplified with *Bam*HI and *Sal*I sites using pCMX-PXR (Dr. Ronald M. Evans, Salk Institute, La Jolla, CA) as the plasmid template with the following primer sequence: forward 5′-accggatcccgatgaagaaggagatgatcatgtcc-3′ and reverse- 5′-agagtcgactcagctacctgtgatgcc-3′. The PCR fragment was subsequently inserted into *Bam*HI and *Sal*I sites of pSH2-1 vector using methods previously published (18, 23). Similarly, full-length SRC-1 was PCR amplified with *Not*I and *Sal*I sites using pCMX-SRC-1 (FL) (amino acids 1–1401) (gift from Drs. Joseph Torchia, University of Western Ontario, London, Ontario, Canada, and Michael G. Rosenfeld, University of California-San Diego, San Diego, CA) (60) as plasmid template with the following primer sequence: forward 5′tatagcggccgcatgagtggcctcggggacagttcatcc3′ and reverse 5′gcggtcgacttattcagtcagtagctg3′. The amplified fragment was subsequently inserted into *Not*I and *Sal*I sites of pGADNot vector. The reactions were carried out in a MasterCycler (Eppendorf, Hamburg, Germany), and the conditions for PCR amplification for both gene products was 94 C for 2 min, followed by 94 C for 45 sec, 55 C for 45 sec, and 72 C for 10 min using PCR Supermix HiFi (Invitrogen, Carlsbad, CA).

Protein-Protein Interaction Assay

To test whether the two-hybrid system would detect human PXR-SRC-1 interaction, two plasmids expressing GAL4-PXR and GAD-SRC-1 fusions were constructed as above. Both plasmids were used to transform strain CTY10-5d, replica plated using nitrocellulose onto drug- and no-drug-containing plates and, upon formation of colonies, examined for production of β-Gal by replicating onto nitrocellulose filters and incubating in buffer containing X-Gal. The colonies turned blue when both expression plasmids were used to cotransform CTY10-5d but not when they were transformed alone. This demonstrated that there was interaction of human PXR and SRC-1 in our yeast two-hybrid system and that the addition of ligand was not necessary for this interaction, presumably because of endogenous yeast compounds that may have served as ligands to human PXR. These methods are in agreement with previously published yeast two-hybrid interactions demonstrated for PXR and SRC-1 (7). Once the assay was established, experiments were repeated in the presence and absence of coumestrol (25 μM).

FP Competition Assays (14)

Antagonists coumestrol and coumestrol diacetate (Sigma) were prepared in buffer A [50 mM phosphate (pH 7.8), 150 mM NaCl, and 5% glycerol] with 25% DMSO. Antagonists for filtered studies were injected through a 0.45-μm nonsterile filter. Filtered and unfiltered antagonist solutions were serially diluted by a factor of two for no less than five dilutions, and 200 nM Flc-labeled SRC-1 peptide (SLTERHKILHRLLQE) (Sigma), 50-fold molar excess of SR12813 (Sigma), and 0.01% Triton were added to each antagonist dilution. A fusion between the PXR LBD and the maltose-binding protein (MBP) was then added according to the K_d established ($\sim$2.6 μM) by a binding assay between PXR-LBD+MBP, SRC-1 peptide, and SR12813. MBP control showed no binding to Flc-labeled peptide. The 50-μl aliquots were added in an enzyme immunoassay/RIA 96-well half-area plate (Costar, Cambridge, MA) and read using a PHERAstar (BMG Labtech) using the FP485, 520A, and 520B filters. Results were analyzed using the four-parameter logistic equation in SigmaPlot. FP values were normalized from 0 (FP value with no protein in buffer A) to 1 (FP value with no antagonist in buffer A).

Competition Ligand-Binding Assays

Full-length human recombinant, histidine-tagged PXR was purchased from PanVera Corp. (Madison, WI; http://www.panvera.com). Purified protein (25 nM) was coated on polylysine SPA beads (Amersham Pharmacia, Piscataway, NJ) and pretreated with BSA to block nonspecific binding sites. NMTB (29) was radiolabeled on the nitrogen with ^{3}H and used as a radioligand (IC_{50} = 3.7 nM in binding assay). The receptor/SPA bead/radioligand mix was added directly to test compounds (coumestrol and SR12813) in the assay plates. Coumestrol and SR12813 were prepared from powder stocks by dissolving in DMSO and diluting in assay buffer [50 mM Tris (pH 8.0), 200 mM KCl, 10% glycerol, 1 mM CHAPS, 0.1 mg/ml BSA, and 2 mM dithiothreitol). Displacement of 10 nM [^{3}H]NMTB was measured in a Wallac Microbeta counter. Nonspecific binding was determined in the presence of 10 μM NMTB. Data were expressed as percent inhibition of bound [^{3}H]NMTB relative to control. The CAR SPA has been described previously (28).

Mass Spectrometry

CV-1 cells were grown in six-well plates in triplicate and scraped on ice. Fifteen strokes were performed using a dounce homogenizer (on ice) (Global Spec Inc., Troy, NY). After a quick spin (10,000 $\times$ *g* for 10 min at 4 C), 5-μl aliquots of CV-1 cell lysates (supernatant) were injected directly into a triple quadrupole mass spectrometer system (QuattroLC; Waters, Milford, MA). The carrier liquid was 50% acetonitrile plus 0.1% formic acid at a flow rate of 0.5 ml/min, provided by a model 515 HPLC pump (Waters), operated isocratically. The electrospray ion source was operated in the negative mode (for compounds of this type of structure, the negative mode provides higher sensitivity than the positive mode). Source temperature was kept at 80 C; the cone voltage was 15 V. Analyte peaks were obtained using the technique of selected reaction monitoring. The following transitions were monitored: m/z from 309–266 for coumestrol diacetate and m/z from 267–182 for coumestrol.

Subnuclear Localization Study Using Confocal Microscopy

HEK293T cells were grown on glass coverslips in six-well plates. After seeding, cells were cotransfected with either 0.5 μg GFP or GFP-PXR along with expression plasmids for SRC-1 or empty vector. After 24 h, cells were treated with 10 μM rifampicin or 0.2% DMSO for 3–4 h in serum-free media. Cells were fixed in 2% paraformaldehyde in PBS for 20 min, mounted with mounting medium that contained 4′,6-diamidino-2-phenylindole, and subjected to confocal microscopy (Olympus CKX41 with filters).

Immunohistochemistry

For tissue specimens, 6-μm-thick frozen sections were cut onto slides using a cryostat, washed with TBS, and then subject to antigen retrieval using pH 6.0 citrate buffer in steamer for 20 min. For immunostaining with human PXR antibodies, tissues were first placed into paraffin blocks, dewaxed with xylene followed by rehydration and antigen retrieval (http://www.ihcworld.com). The tissue/cells were

then sequentially blocked with 5% rabbit serum/2% BSA/0.1% Triton X-100 for 60 min at room temperature. Tissues were incubated with a 1:40 dilution of the primary polyclonal human PXR antibody (Biolegend, Inc., San Diego, CA) or a 1:100 dilution of mouse PXR antibody (R-14; Santa Cruz Biotechnology, Santa Cruz, CA) for 12 h or at 4 C overnight followed by the biotinylated secondary antibody for 1 h. Cell sections were then immunostained with the biotin-streptavidin system from Vector Laboratories (Burlingame, CA) per the manufacturer's instructions. Hematoxylin and eosin (H&E) stains were performed on frozen sections using routine methods (http://www.histosearch.com). For controls, tissues were incubated without primary antibody or with PXR protein (hemagglutinin-tagged) in the presence of primary antibody.

Primary Culture of Human Hepatocytes and RNA Analysis

Primary human hepatocytes were obtained from Biowhittaker (East Rutherford, NJ). Cells were cultured in Matrigel-coated six-well plates in serum-free William's E medium (Life Technologies, Rockville, MD) supplemented with 100 nM dexamethasone and insulin-transferrin-selenium (ITS-G; Life Technologies). At 48 h after isolation, hepatocytes were treated with bisphosphonate ester SR12813 (1 μM), rifampicin (10 μM), and/or coumestrol (25 μM), which were added to the culture medium as 1000× stocks in DMSO. Control cultures received vehicle alone. Cells were cultured for an additional 48 h with drug treatments repeated at 24 h to refresh media and compounds. RNA was isolated using Trizol (Life Technologies) according to the manufacturer's instructions. Total RNA (10 mg) was resolved using a 1% agarose/2.2 M formaldehyde denaturing gel and transferred to a nylon membrane (Hybond N+; Amersham Pharmacia). Blots were hybridized sequentially with ^{32}P-labeled *CYP3A4* (bases 790-1322 of the published cDNA sequence, GenBank accession no. M18907), *CYP2B6* (bases 7–1527 of the published cDNA sequence, Genbank accession no. NM_009998), and β-actin (Clontech) probes.

Animal Treatment and LORR Studies in PXR (+/+), Humanized PXR, and PXR (−/−) Mice

Adult female PXR wild-type and PXR (−/−) mice were maintained on standard laboratory chow and were allowed food and water *ad libitum*. Mice (n = 5 per treatment group) were treated with either corn oil vehicle (d 1–6), PCN (150 mg/kg·d ip, d 3–6), coumestrol (100 mg/kg·d divided three times per day sc, d 1–6), coumestrol diacetate (100 mg/kg·d divided three times per day sc, d 1–6), or the combination of the same dose/schedule of PCN and coumestrol or coumestrol diacetate. On d 3 and 6, LORR studies were performed as previously published (23). All animal experimentation described in the submitted manuscript was conducted in accord with accepted standards of humane animal care, as outlined in the National Institutes of Health Guide for the Care and Use of Laboratory Animals.

Acknowledgments

Received April 26, 2007. Accepted December 14, 2007.

Address all correspondence and requests for reprints to: Sridhar Mani, Albert Einstein College of Medicine, 1300 Morris Park Avenue, Bronx, New York 10461. E-mail: smani@montefiore.org.

This work was supported by a grant from the Damon Runyon Cancer Research Foundation (CI: 15-02 to S.M.).

Disclosure Statement: H.W., H.L., M.D.L.J., G.V.K., M.V., W.X., S.Y.C., J.R., M.R., and S.M. have nothing to declare. L.B.M., J.M.M., B.G., O.R.R.I., B.W., K.C., D.J.P., J.L.C., T.M.W., and J.T.M. are employees of GlaxoSmithKline.

REFERENCES

1. Staudinger JL, Goodwin B, Jones SA, Hawkins-Brown D, MacKenzie KI, LaTour A, Liu Y, Klaassen CD, Brown KK, Reinhard J, Willson TM, Koller BH, Kliewer SA 2001 The nuclear receptor PXR is a lithocholic acid sensor that protects against liver toxicity. Proc Natl Acad Sci USA 98:3369–3374
2. Liddle C, Goodwin B 2002 Regulation of hepatic drug metabolism: role of the nuclear receptors PXR and CAR. Semin Liver Dis 22:115–122
3. Moore JT, Kliewer SA 2000 Use of the nuclear receptor PXR to predict drug interactions. Toxicology 153:1–10
4. Xie W, Radominska-Pandya A, Shi Y, Simon CM, Nelson MC, Ong ES, Waxman DJ, Evans RM 2001 An essential role for nuclear receptors SXR/PXR in detoxification of cholestatic bile acids. Proc Natl Acad Sci USA 98: 3375–3380
5. Xie W, Barwick JL, Downes M, Blumberg B, Simon CM, Nelson MC, Neuschwander-Tetri BA, Brunt EM, Guzelian PS, Evans RM 2000 Humanized xenobiotic response in mice expressing nuclear receptor SXR. Nature 406: 435–439
6. Goodwin B, Gauthier KC, Umetani M, Watson MA, Lochansky MI, Collins JL, Leitersdorf E, Mangelsdorf DJ, Kliewer SA, Repa JJ 2003 Identification of bile acid precursors as endogenous ligands for the nuclear xenobiotic pregnane X receptor. Proc Natl Acad Sci USA 100: 223–228
7. Masuyama H, Suwaki N, Tateishi Y, Nakatsukasa H, Segawa T, Hiramatsu Y 2005 The pregnane X receptor regulates gene expression in a ligand- and promoter-selective fashion. Mol Endocrinol 19:1170–1180
8. Maglich JM, Stoltz CM, Goodwin B, Hawkins-Brown D, Moore JT, Kliewer SA 2002 Nuclear pregnane x receptor and constitutive androstane receptor regulate overlapping but distinct sets of genes involved in xenobiotic detoxification. Mol Pharmacol 62:638–646
9. Xue Y, Moore LB, Orans J, Peng L, Bencharit S, Kliewer SA, Redinbo MR 2007 Crystal structure of the pregnane X receptor-estradiol complex provides insights into endobiotic recognition. Mol Endocrinol 21:1028–1038
10. Mnif W, Pascussi JM, Pillon A, Escande A, Bartegi A, Nicolas JC, Cavailles V, Duchesne MJ, Balaguer P 2007 Estrogens and antiestrogens activate hPXR. Toxicol Lett 170:19–29
11. Watkins RE, Davis-Searles PR, Lambert MH, Redinbo MR 2003 Coactivator binding promotes the specific interaction between ligand and the pregnane X receptor. J Mol Biol 331:815–828
12. Watkins RE, Noble SM, Redinbo MR 2002 Structural insights into the promiscuity and function of the human pregnane X receptor. Curr Opin Drug Discov Dev 5:150–158
13. Watkins RE, Wisely GB, Moore LB, Collins JL, Lambert MH, Williams SP, Willson TM, Kliewer SA, Redinbo MR 2001 The human nuclear xenobiotic receptor PXR: structural determinants of directed promiscuity. Science 292: 2329–2333
14. Ozers MS, Ervin KM, Steffen CL, Fronczak JA, Lebakken CS, Carnahan KA, Lowery RG, Burke TJ 2005 Analysis of ligand-dependent recruitment of coactivator peptides to estrogen receptor using fluorescence polarization. Mol Endocrinol 19:25–34
15. Xue Y, Chao E, Zuercher WJ, Willson TM, Collins JL, Redinbo MR 2007 Crystal structure of the PXR-T1317 complex provides a scaffold to examine the potential for receptor antagonism. Bioorg Med Chem 15:2156–2166
16. Shiau AK, Barstad D, Loria PM, Cheng L, Kushner PJ, Agard DA, Greene GL 1998 The structural basis of estrogen receptor/coactivator recognition and the antagonism of this interaction by tamoxifen. Cell 95:927–937

17. Mahfoudi A, Roulet E, Dauvois S, Parker MG, Wahli W 1995 Specific mutations in the estrogen receptor change the properties of antiestrogens to full agonists. Proc Natl Acad Sci USA 92:4206–4210
18. Wang H, Huang H, Li H, Teotico DG, Sinz M, Baker SD, Staudinger J, Kalpana G, Redinbo MR, Mani S 2007 Activated pregnenolone X-receptor is a target for ketoconazole and its analogs. Clin Cancer Res 13:2488–2495
19. Arnold LA, Estébanez-Perpiñá E, Togashi M, Shelat A, Ocasio CA, McReynolds AC, Nguyen P, Baxter JD, Fletterick RJ, Webb P, Guy RK 2006 A high-throughput screening method to identify small molecule inhibitors of thyroid hormone receptor coactivator binding. Sci STKE 341:13
20. Zhou C, Poulton EJ, Grun F, Bammler TK, Blumberg B, Thummel KE, Eaton DL 2007 The dietary isothiocyanate sulforaphane is an antagonist of the human steroid and xenobiotic nuclear receptor. Mol Pharmacol 71:220–229
21. Synold TW, Dussault I, Forman BM 2001 The orphan nuclear receptor SXR coordinately regulates drug metabolism and efflux. Nat Med 7:584–590
22. Takeshita A, Taguchi M, Koibuchi N, Ozawa Y 2002 Putative role of the orphan nuclear receptor SXR (steroid and xenobiotic receptor) in the mechanism of CYP3A4 inhibition by xenobiotics. J Biol Chem 277:32453–32458
23. Huang H, Wang H, Sinz M, Zoeckler M, Staudinger J, Redinbo MR, Teotico DG, Locker J, Kalpana GV, Mani S 2006 Inhibition of drug metabolism by blocking the activation of nuclear receptors by ketoconazole. Oncogene 26:258–268
24. Whitten PL, Patisaul HB 2001 Cross-species and interassay comparisons of phytoestrogen action. Environ Health Perspect 109:5–20
25. Shan L, Vincent J, Brunzelle JS, Dussault I, Lin M, Ianculescu I, Sherman MA, Forman BM, Fernandez EJ 2004 Structure of the murine constitutive androstane receptor complexed to androstenol: a molecular basis for inverse agonism. Mol Cell 16:907–917
26. Moore LB, Maglich JM, McKee DD, Wisely B, Willson TM, Kliewer SA, Lambert MH, Moore JT 2002 Pregnane X receptor (PXR), constitutive androstane receptor (CAR), and benzoate X receptor (BXR) define three pharmacologically distinct classes of nuclear receptors. Mol Endocrinol 16:977–986
27. Jones SA, Moore LB, Shenk JL, Wisely GB, Hamilton GA, McKee DD, Tomkinson NC, LeCluyse EL, Lambert MH, Willson TM, Kliewer SA, Moore JT 2000 The pregnane X receptor: A promiscuous xenobiotic receptor that has diverged during evolution. Mol Endocrinol 14:27–39
28. Moore LB, Parks DJ, Jones SA, Bledsoe RK, Consler TG, Stimmel JB, Goodwin B, Liddle C, Blanchard SG, Willson TM, Collins JL, Kliewer SA 2000 Orphan nuclear receptors constitutive androstane receptor and pregnane X receptor share xenobiotic and steroid ligands. J Biol Chem 275:15122–15127
29. Schultz JR, Tu H, Luk A, Repa JJ, Medina JC, Li L, Schwendner S, Wang S, Thoolen M, Mangelsdorf DJ, Lustig KD, Shan B 2000 Role of LXRs in control of lipogenesis. Genes Dev 14:2831–2838
30. Chrencik JE, Orans J, Moore LB, Xue Y, Peng L, Collins JL, Wisely GB, Lambert MH, Kliewer SA, Redinbo MR 2005 Structural disorder in the complex of human pregnane X receptor and the macrolide antibiotic rifampicin. Mol Endocrinol 19:1125–1134
31. Kawana K, Ikuta T, Kobayashi Y, Gotoh O, Takeda K, Kawajiri K 2003 Molecular mechanism of nuclear translocation of an orphan nuclear receptor, SXR. Mol Pharmacol 63:524–531
32. Bhalla S, Ozalp C, Fang S, Xiang L, Kemper JK 2004 Ligand-activated pregnane X receptor interferes with HNF-4 signaling by targeting a common coactivator PGC-1α. Functional implications in hepatic cholesterol and glucose metabolism. J Biol Chem 279:45139–45147
33. Szkudelska K, Szkudelski T, Nogowski L 2002 Daidzein, coumestrol and zearalenone affect lipogenesis and lipolysis in rat adipocytes. Phytomedicine 9:338–345
34. Code EL, Crespi CL, Penman BW, Gonzalez FJ, Chang TK, Waxman DJ 1997 Human cytochrome P4502B6: interindividual hepatic expression, substrate specificity, and role in procarcinogen activation. Drug Metab Dispos 25:985–993
35. Gibson GG, Plant NJ, Swales KE, Ayrton A, El-Sankary W 2002 Receptor-dependent transcriptional activation of cytochrome P4503A genes: induction mechanisms, species differences and interindividual variation in man. Xenobiotica 32:165–206
36. Bulayeva NN, Watson CS 2004 Xenoestrogen-induced ERK-1 and ERK-2 activation via multiple membrane-initiated signaling pathways. Environ Health Perspect 112: 1481–1487
37. Kodama S, Koike C, Negishi M, Yamamoto Y 2004 Nuclear receptors CAR and PXR cross talk with FOXO1 to regulate genes that encode drug-metabolizing and gluconeogenic enzymes. Mol Cell Biol 24:7931–7940
38. Rice S, Whitehead SA 2006 Phytoestrogens and breast cancer: promoters or protectors? Endocr Relat Cancer 13:995–1015
39. Jonas BA, Privalsky ML 2004 SMRT and N-CoR corepressors are regulated by distinct kinase signaling pathways. J Biol Chem 279:54676–54686
40. Hong SH, Privalsky ML 2000 The SMRT corepressor is regulated by a MEK-1 kinase pathway: inhibition of corepressor function is associated with SMRT phosphorylation and nuclear export. Mol Cell Biol 20:6612–6625
41. Asada S, Daitoku H, Matsuzaki H, Saito T, Sudo T, Mukai H, Iwashita S, Kako K, Kishi T, Kasuya Y, Fukamizu A 2007 Mitogen-activated protein kinases, Erk and p38, phosphorylate and regulate Foxo1. Cell Signal 19: 519–527
42. Zhu Z, Kim S, Chen T, Lin JH, Bell A, Bryson J, Dubaquie Y, Yan N, Yanchunas J, Xie D, Stoffel R, Sinz M, Dickinson K 2004 Correlation of high-throughput pregnane X receptor (PXR) transactivation and binding assays. J Biomol Screen 9:533–540
43. Moore LB, Goodwin B, Jones SA, Wisely GB, Serabjit-Singh CJ, Willson TM, Collins JL, Kliewer SA 2000 St. John's wort induces hepatic drug metabolism through activation of the pregnane X receptor. Proc Natl Acad Sci USA 97:7500–7502
44. Piscitelli SC, Burstein AH, Chaitt D, Alfaro RM, Falloon J 2000 Indinavir concentrations and St John's wort. Lancet 355:547–548
45. Ruschitzka F, Meier PJ, Turina M, Luscher TF, Noll G 2000 Acute heart transplant rejection due to Saint John's wort. Lancet 355:548–549
46. Laakmann G, Schule C, Baghai T, Kieser M 1998 St. John's wort in mild to moderate depression: the relevance of hyperforin for the clinical efficacy. Pharmacopsychiatry 31:54–59
47. Ernst E, Rand JI, Barnes J, Stevinson C 1998 Adverse effects profile of the herbal antidepressant St. John's wort (*Hypericum perforatum* L.). Eur J Clin Pharmacol 54:589–594
48. Blumberg B, Sabbagh Jr W, Juguilon H, Bolado Jr J, van Meter CM, Ong ES, Evans RM 1998 SXR, a novel steroid and xenobiotic-sensing nuclear receptor. Genes Dev 12: 3195–3205
49. Humphreys CD 1998 Phytoestrogens and human health effects: weighing up the current evidence. Nat Toxins 6:1–59
50. Willson TM, Cobb JE, Cowan DJ, Wiethe RW, Correa ID, Prakash SR, Beck KD, Moore LB, Kliewer SA, Lehmann JM 1996 The structure-activity relationship between peroxisome proliferator-activated receptor γ agonism and the antihyperglycemic activity of thiazolidinediones. J Med Chem 39:665–668

51. Northrop JP, Nguyen D, Piplani S, Olivan SE, Kwan ST, Go NF, Hart CP, Schatz PJ 2000 Selection of estrogen receptor β- and thyroid hormone receptor β-specific coactivator-mimetic peptides using recombinant peptide libraries. Mol Endocrinol 14:605–622
52. Mangelsdorf DJ, Umesono K, Kliewer SA, Borgmeyer U, Ong ES, Evans RM 1991 A direct repeat in the cellular retinol-binding protein type II gene confers differential regulation by RXR and RAR. Cell 66:555–561
53. Goodwin B, Hodgson E, Liddle C 1999 The orphan human pregnane X receptor mediates the transcriptional activation of CYP3A4 by rifampicin through a distal enhancer module. Mol Pharmacol 56:1329–1339
54. Henke BR, Consler TG, Go N, Hale RL, Hohman DR, Jones SA, Lu AT, Moore LB, Moore JT, Orband-Miller LA, Robinett RG, Shearin J, Spearing PK, Stewart EL, Turnbull PS, Weaver SL, Williams SP, Wisely GB, Lambert MH 2002 A new series of estrogen receptor modulators that display selectivity for estrogen receptor β. J Med Chem 45:5492–5505
55. Gietz RD, Sschiestl RH 1991 Applications of high efficiency lithium acetate transformation of intact yeast cells using single-stranded nucleic acids as carrier. Yeast 7:253–263
56. Gietz RD, Woods RA 2002 Sreening for protein-protein interactions in the yeast two-hybrid system. Methods Mol Biol 185:471–486
57. Kalpana GV, Goff SP 1993 Genetic analysis of homomeric interactions of human immunodeficiency virus type 1 integrase using the yeast two-hybrid system. Proc Natl Acad Sci USA 90:10593–10597
58. Hanes SD, Brent R 1989 DNA specificity of the bicoid activator protein is determined by homeodomain recognition helix residue 9. Cell 57:1275–1283
59. Luban J BK, Franke EK, Kalpana GV, Goff SP 1993 Human immunodeficiency virus type 1 Gag protein binds to cyclophilins A and B. Cell 73:1067–1078
60. Torchia J, Rose DW, Inostroza J, Kamei Y, Westin S, Glass CK, Rosenfeld MG 1997 The transcriptional coactivator p/CIP binds CBP and mediates nuclear-receptor function. Nature 387:677–684

Molecular Endocrinology **is published monthly by The Endocrine Society (http://www.endo-society.org), the foremost professional society serving the endocrine community.**